

Orbital contributions to the exchange-repulsion energy of atomic and molecular aggregates

Bachelorarbeit der Mathematisch-Naturwissenschaftlichen Fakultät der
EBERHARD-KARLS UNIVERSITÄT TÜBINGEN im Fach Chemie

angefertigt im Sommersemester 2018

im Arbeitskreis Prof. Dr. Reinhold F. Fink

vorgelegt von

Gemma Miralles Adrover



EBERHARD KARLS
UNIVERSITÄT
TÜBINGEN



Tübingen, Juni 2018

Declaration

Hereby I declare:

- that I wrote this work myself and I did not use any sources other than those indicated.
- that I have observed the guidelines for securing good scientific practice and dealing with scientific misconduct at Eberhard-Karls-Universität.
- that the submitted work was neither completely nor in substantial part subject to another examination procedure.

Tübingen, May 28, 2018



Gemma Miralles Adrover

Index

1. Abstract.....	3
2. Introduction	4
3. Objective.....	5
4. Theoretical Background	6
4.1 Hartree-Fock method	6
4.2 Density functional theory	6
4.3 Basis sets.....	7
4.3.1 Type of basis sets.....	7
4.3.2 Basis sets used.....	8
4.4 Orbital pair contributions to the exchange-repulsion energy.....	9
4.4.1 The exchange-repulsion energy.....	9
4.5 Energy decomposition analysis (EDA) of covalent bonds and intermolecular interactions	10
4.5.1 Hartree Fock interaction	11
4.5.2 Kohn-Sham method	12
5. E_{ext} calculation in $\text{N}_2\text{-He}$ and $\text{Cl}_2\text{-He}$ systems.....	13
5.1 Computational details.....	13
5.2 $\text{N}_2\text{-He}$ System.....	13
5.2.1 Description of the system	13
5.2.2 Orbitals studied	14
5.2.3 Basis sets quality	15
5.2.4 Results and discussion	16
5.3 $\text{Cl}_2\text{-He}$ System	18
5.3.1 Description of the system	18
5.3.2 Orbitals studied	19
5.3.3 Basis sets quality	20
5.3.4. Results and discussion.....	21
6. Energy decomposition analysis	23
6.1 Computational details.....	23
6.2 $\text{N}_2\text{-He}$	23
6.2.1 Description of the system	23
6.2.2 Basis sets quality	24
6.2.3 HF calculation.....	24

6.2.4 DFT calculation	25
6.3 Cl ₂ -He	26
6.3.1 Description of the system	26
6.3.2 HF calculation.....	26
6.3.3 DFT calculation	28
7. 2D Calculation	30
7.2. Computational details.....	30
7.3. N ₂ -He	30
7.3.1 Description of the system	30
7.3.2 Results	31
7.4 Cl ₂ -He	31
7.4.1Description of the system	31
7.4.2 Results	31
8. Introduction to Perylene Bisimides	32
8.1 Description of the system	33
8.2 Computational details.....	33
8.3 Orbitals studied	33
8.4 Results when PBI2 is shifted along the z-axis.....	35
8.5 Results when PBI2 is shifted along the y-axis.....	37
9. Conclusions.....	39
10. Bibliography	41
Appendix	42
Acknowledgements	46

1. Abstract

English

The exchange-repulsion energy (E_{exr}) has been calculated for horizontal displacements of three different systems: $\text{N}_2\text{-He}$, $\text{Cl}_2\text{-He}$ and the perylene bisimide (PBI) dimer. The calculations were carried out with different basis sets: TZVP, cc-pVDZ, cc-pVTZ and aug-cc-pVDZ for the two smaller systems and TZVP for the larger system PBI-PBI. The aim of these calculations is to determine the interactions of the orbitals that contribute most to the E_{exr}

Additionally, the interaction energy contributions between a Helium atom and a N_2 as well as a Cl_2 molecule were determined with an energy decomposition analysis (EDA). The calculations were performed in horizontal and vertical displacements of the He using HF and DFT methods (in the latter B-LYP was used as functional) together with the same basis set previously mentioned.

The purpose of this part was dedicated to studying the contribution of each type of energy to the total interaction energy of the system (E_{int}). It has been observed that the E_{exr} has a fair if not the most important contribution to the total energy.

Finally, an HF 2D calculation has also been performed too on the $\text{N}_2\text{-He}$ and $\text{Cl}_2\text{-He}$ systems with TZVP as a basis set. Here, energy isocontours have been observed to a better understanding of the interactions of both monomers.

Català

L'energia de bescanvi-repulsió (E_{exr}) s'ha calculat per a desplaçaments horitzontals en tres sistemes diferents: $\text{N}_2\text{-He}$, $\text{Cl}_2\text{-He}$ i el dímer de perilè bisimida (PBI). En els dos primers sistemes els càlculs s'han realitzat amb diferents conjunts de bases: TZVP, cc-pVDZ, cc-pVTZ i aug-cc-pVDZ per als dos sistemes petits i TZVP per al sistema més gran PBI-PBI. En aquests càlculs s'han determinat les interaccions dels orbitals que contribueixen més a l' E_{exr} i quin és el seu valor en determinats punts.

També s'ha dut a terme el càlcul de les energies derivades d'una anàlisi de descomposició d'energia (EDA) per als sistemes $\text{N}_2\text{-He}$ i $\text{Cl}_2\text{-He}$. Els càlculs s'han realitzat en desplaçaments horitzontals i verticals de l'He mitjançant el mètode HF i DFT amb B-LYP com a funcional de densitat i amb les mateixes bases anomenades anteriorment. En aquests càlculs s'ha observat com contribueix cada energia a l'energia d'interacció total (E_{int}) entre molècules i s'ha pogut observar que E_{exr} és l'energia que contribueix més a E_{int} .

Finalment, també s'ha dut a terme un càlcul HF 2D en els sistemes $\text{N}_2\text{-He}$ i $\text{Cl}_2\text{-He}$ amb TZVP com a base. Aquí s'han observat isocontorns d'energia per entendre millor les interaccions entre els dos monòmers.

2. Introduction

Nowadays, the situation on our planet makes us consider how much longer we can continue to exploit the natural resources in order to obtain energy. Unfortunately, the contemporary energy production is mostly based on a larger non-renewable energy sources, such as fossil fuels or nuclear energy (on a smaller scale). However, we have reached a point in which society has to be aware of it due to the negative environmental impact that its use implies and which are limited to the planet.

Accordingly, with the growth and development of new technologies, science and technology have to collaborate together in order to face the problem of the energy crisis. The role of chemistry is very important in order to generate appropriate materials, which causes computational chemistry to play an important role in researching and evolving in the field of renewable energies.

One of the main renewable energies is solar cells, which can transform the sun's luminous energy into electrical energy. Quantum chemistry developed methods to understand and improve this transformation of energy.

Conventional solar cells are based on silicon, but nowadays, dye-sensitive solar cells are being investigated, which are an alternative to the conventional ones due to their low production cost, easy manufacturing, and advantageous optical properties.

In these solar cells, organic molecules absorb sunlight. Therefore, computational methods are used to predict optical properties (UV, absorption wave, etc.) of these molecules. These data provide information when designing and improving solar cells.

Perylene bisimides (PBI) represent a class of well-established and robust organic dye molecules, which are studied in this work with simpler systems such as N_2 -He and Cl_2 -He^{[1],[2]}. Here, the exchange-repulsion energy is calculated to study the interaction of the orbitals of the two subsystems (molecules A and B) considered. The repulsion energy is investigated with a newly developed approach that allows to expand this interaction in terms of each occupied orbital of one monomer with each orbital one of the other.

3. Objective

In this work, there are three systems studied: N₂-He, Cl₂-He, and PBI. The objectives are the following

- In N₂-He and Cl₂-He systems:
 - Calculate the exchange-repulsion energy (E_{exr}) in horizontal and vertical displacements using the Hartree-Fock method.
 - Determine the orbital contributions to E_{exr} .
 - Calculate the interaction energy contributions as obtained from an energy decomposition analysis (EDA) using the HF and B-LYP methods.
 - Check the extend of E_{exr} to the total interaction energy (E_{int}).
 - Perform all previous calculations with different basis sets (TZVP, cc-pVDZ, cc-pVTZ, and aug-cc-pVDZ) to observe which basis set is required to obtain reliable results.
 - Calculate E_{exr} in a two dimensional plane that includes the atomic positions of N₂ (Cl₂) to obtain a complete picture of the exchange-repulsion interactions between both monomers.

- In the PBI-PBI system:
 - Calculate the exchange-repulsion energy (E_{exr}) in horizontal and vertical displacements using HF method.
 - Observe which are the orbitals that contribute most to the E_{exr} and see how they interact.

4. Theoretical Background

4.1 Hartree-Fock method

A major goal of the computational chemistry methods is solving the Schrödinger equation. To solve this equation, the Born–Oppenheimer approximation, where the coupling between the nuclei and electronic motion is neglected, is considered. This allows the electronic part to be solved with the nuclear positions as parameters, and the resulting potential energy surface (PES) forms the basis for solving the nuclear motion.

The Hartree-Fock (HF) ^{[3][4]} method solves approximately the electronic Schrödinger equation. As the dynamics of a many-electron system is very complex, a simplification is made, both computationally and conceptually. This approximation consists of introducing independent-particle models, where the motion of one electron is considered to be independent of the dynamics of all other electrons. In the HF method, an independent-particle model means that the motion of an electron and the field of the others is approximated by taking all interactions into account in an average fashion.

Moreover, in this model, each electron is described by an orbital, and the total wave function is given as an antisymmetrized product of orbitals called Slater determinant, which is made up of one spin-orbital per electron. The variational principle is used to minimizing the energy expectation value of the Slater determinant leading to the HF equations.

The HF model typically accounts for ~99% of the total energy, but the remaining correlation energy is usually very important for chemical purposes. The correlation between the electrons describes the “wiggles” relative to the HF orbitals due to the instantaneous interaction between the electrons, rather than just the average repulsion. The goal of correlated methods for solving the Schrödinger equation is to calculate the remaining correction due to the electron-electron interaction.

4.2 Density functional theory

Density functional theory (DFT) ^{[3][5]} is a popular ab initio method. It is based on a theorem of Hohenberg and Kohn (1964), which states that a knowledge of the electron density of a system in its ground state is enough to determine the energy: “the energy is a functional of the density”. An informal understanding provided by Wilson (1968) claims that the exact density has cusps only at the positions of the nuclei, and the gradient of the density at the cusp depends on the nuclear charge. Moreover the integral of the density of all spaces gives the number of electrons. A knowledge of the density, therefore, allows one to write the Hamiltonian, from which everything can be determined. This also illustrates that although the theorem is rigorous, it does not in itself provide a practical way to calculate the energy from a given density. The literature contains many proposed functionals which may be used for this purpose, but at the present time, the exact functional is not known. The functionals in current use are based on the theory of the uniform electron gas, together with various limiting properties that the functional must satisfy ^[5].

DFT in the Kohn–Sham version can be considered as an improvement on HF theory, where the many-body effect of electron correlation is modelled by a function of the electron density. DFT is, analogously to HF, an independent-particle model, and is comparable to HF computationally, but provides significantly better results. The main disadvantage of DFT is that there is no systematic approach to improving the results towards the exact solution ^[3].

The functional used in this work is B-LYP, which is a combination of the LYP correlation functional with the B88 exchange functional.

4.3 Basis sets

The computational methods used in this work are *ab initio* methods, which try to solve the Schrödinger or Kohn-Sham equation. An approximation inherent in essentially all these methods is the introduction of a basis set ^[3]. The latter is used to expand an unknown function, such as a molecular orbital. If the basis set is complete, it is not an approximation. However, a complete basis set means that an infinite number of functions must be used, which is not possible in calculations.

The type and number of basis functions used influence the accuracy. The better a single basis function is able to reproduce the unknown function, the fewer basis functions are necessary for achieving a given level of accuracy. Generally, it can be stated that the smaller (better) the basis set, the poorer (more appropriate) the representation of the orbitals.

4.3.1 Type of basis sets

There are two types of basis functions (also called Atomic Orbitals) used in electronic structure calculations: Slater Type Orbitals (STO) and Gaussian Type Orbitals (GTO).

STOs are primarily used for atomic and diatomic systems where high accuracy is required. Both STOs and GTOs can be chosen to form a complete basis, but more GTOs are necessary for achieving a certain accuracy compared with STOs. Roughly three times as many GTOs as STOs are required for reaching a given level of accuracy.

In terms of computational efficiency, GTOs are preferred and are more used as basis functions in electronic structure calculations, even the GTO basis functions have to be increased. The location of the functions is also important. For example, for certain types of calculations, the centre of a basis function may be taken not to coincide with a nucleus, for example being placed at the centre of a bond or between non-bonded atoms for improving the calculation of van der Waals interactions.

The functions of the basis sets used are GTO's.

GTO basis sets can be written in terms of polar or Cartesian coordinates as shown in the following equations

$$X_{\zeta n,l,m}(r, \theta, \varphi) = NY_{l,m}(\theta, \varphi) r^{2n-2-l} e^{-\zeta r^2} \quad (1)$$

$$X_{\zeta,l_x,l_y,l_z} = Nx^{l_x}y^{l_y}z^{l_z}e^{-\zeta r^2} \quad (2)$$

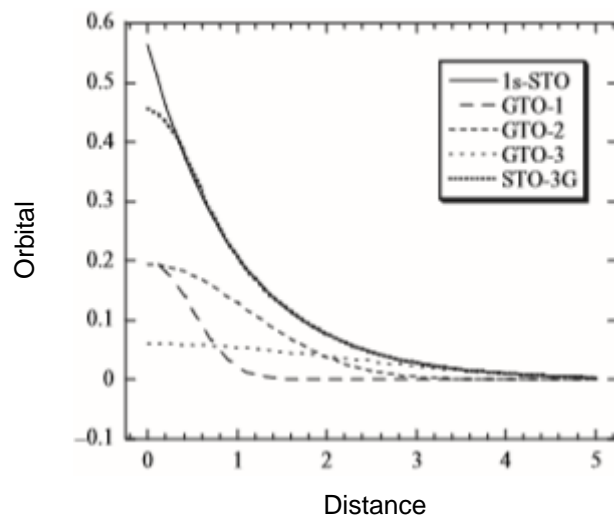


Illustration 1. A 1s-STO modelled by a linear combination of three GTOs (STO-3G). (taken from reference [3]).

GTOs have worse representation than STOs due to the r^2 dependency in the exponential. At the nucleus, a GTO has a zero slope, in contrast to an STO which has a “cusp” (discontinuous derivative). GTOs have also problems representing the proper behaviour near the nucleus. Furthermore, compared with an STO, GTO falls off too rapidly far from the nucleus, and the “tail” of the wave function is consequently represented poorly. Both STOs and GTOs can be chosen to form a complete basis, but more GTOs are necessary for achieving a certain accuracy [3].

3.3.2 Basis sets used

The basis sets used [3],[6] in this work are the following

- TZVP (Triple Zeta Split Valence Polarized). The term TZ means that this basis contains three times as many functions as the minimum basis, i.e. six s-functions and three p-functions for the first row elements. The term V means that the only orbitals which are triplicated are the valence orbitals. The core orbitals are contracted. The P allows the movement of the orbitals of an atom as other atoms approach. For example, an orbital can be polarized in one direction if it is mixed with a p orbital.
- cc-pVDZ (correlation consistent Polarized Valence Double Zeta). The correlation consistent basis sets aim to recover the correlation energy of the valence electrons. The name correlation consistent refers to the fact that the basis sets

are designed such that functions that contribute similar amounts of correlation energy are included at the same stage, independent of the function type. Several different sizes of cc basis sets are available in terms of final number of contracted functions.

- cc-pVTZ (correlation consistent Polarized Valence Triple Zeta). It is the same as the previous one, but this basis set triples the number of valence orbitals.
- aug-cc-pVDZ (augmented correlation consistent Polarized Valence Double Zeta). The prefix “aug” refers to the energy-optimized in cc-basis sets can be augmented with diffuse functions. The augmentation consists of adding one extra function with a smaller exponent for each angular momentum. The aug-cc-pVDZ has additionally one s-, one p- and one d-function.

3.4 Orbital pair contributions to the exchange-repulsion energy

3.4.1 The exchange-repulsion energy

The interaction energy of molecules is dominated by (i) electrostatic interactions (ii) London dispersion and (iii) Pauli repulsion. Additionally, induction and charge transfer play a role as well as covalent contributions. For polar molecules, the electrostatic interaction is in many cases strongly determining the actual structure of aggregates and crystals. Furthermore, electrostatic interactions are bonding and non-bonding as a function of the intermolecular arrangement, while dispersion is always attractive and more isotropic while Pauli repulsion is exclusively repulsive [7]. Due to its quantum mechanical character and its not yet perfectly understood nature, the Pauli repulsion will be studied in this work.

The exchange-repulsion energy [5], [7] is a combination of two effects. The ‘exchange’ energy is a consequence of the fact that the electron motions can extend over both molecules, and is an attractive term, while the “repulsion” energy is a repulsive term that arises when the electrons attempt to occupy the same region of space, and are forced to redistribute because the Pauli principle forbids electrons of the same spin to be in the same place [5].

According to reference [7], for a dimer system described with the Hartree-Fock orbitals a , a' , ... and b , b' , ... of the two monomers, respectively, the exchange and repulsion energies contributions to the dimer are

$$E_{exc}(a, b) = -\sum_{ab} 2(ab|ba) \quad (3)$$

$$E_{rep}(a, b) = \sum_{ij} 2(i|\hat{V}_A + \hat{V}_B + \hat{T}|j)[(S^{-1})_{ji} - \delta_{ji}] + \sum_{ijkl} [2(ij|kj) - (il|kl)] [(S^{-1})_{ji} (S^{-1})_{lk} - \delta_{ji} \delta_{lk}] \quad (4)$$

Here \hat{V}_A and \hat{V}_B are the nuclear attraction operators comprising all nuclei at molecule A and B respectively, \hat{T} is the kinetic energy operator, (ij|kl) a two electron integral in charge density (Mulliken) notation with i, j, k, l standing for all orbitals in the dimer system and S^{-1} is the inverse of the overlap matrix between the occupied orbitals in the two systems.

The Pauli repulsion energy can be approximately rewritten in a sum of orbital contributions

$$E''_{Pauli} = \sum_{a,b} E''_{Pauli}(a, b) \quad (5)$$

Where the orbital contribution to the repulsion energy is given by

$$E''_{Pauli}(a, b) = 2 S_{ba} \{[(\epsilon_a + \epsilon_b)S_{ab} - 2(a|\hat{F}_A + \hat{F}_B|b) + 2T_{ab}] + \sum_{a'}(a|v_B|a')S_{a'b} + \sum_{a'}(b|v_A|b')S_{b'a} - \sum_{a'b'}(aa'|bb')S_{b'a'}\} \quad (6)$$

Here \hat{F}_A and \hat{F}_B corresponds to the Fock operators of systems A and B. ϵ_a and ϵ_b are the eigenvalues of the Fock operators.

The exchange term generally shows a similar asymptotic behaviour as the Pauli-repulsion. Hence, is common to add the exchange interaction to the Pauli term in order to obtain the “exchange-repulsion” energy. The orbital contribution to the exchange repulsion energy is thus written as

$$E_{exr}(a, b) = E_{exc}(a, b) + E''_{Pauli}(a, b) \quad (7)$$

Exchange-repulsion interaction only arises if two electrons have the same spin. If they have opposite spins, chemical bonding could occur. In an interaction between two closed-shell molecules, as in the presently investigated cases, this is not possible.

3.5 Energy decomposition analysis (EDA) of covalent bonds and intermolecular interactions

Intermolecular interaction plays an important role in determining the aggregation structures of condensed molecular systems. The knowledge of the total intermolecular interaction energy is often desirable to understand chemical and physical properties [8]. The lower the total intermolecular interaction energy, the more stable the structure of the system will be.

In this work, the EDA in the HF and DFT calculations are based on the work of Su and Li [8a]. For HF methods, the total interaction energy from a supermolecule calculation is decomposed into electrostatic, exchange, repulsion and polarization terms. For Kohn-Sham density functional interaction energy is decomposed into electrostatic, exchange, repulsion, polarisation and dispersion terms.

3.5.1 Hartree Fock interaction

For a supermolecule X consisting of monomers A, the total HF interaction energy is

$$\Delta E^{HF} = \langle \phi_X | H_X | \phi_X \rangle - \sum_A \langle \phi_A | H_A | \phi_A \rangle \quad (8)$$

Where ϕ_X and ϕ_A are the variational single-determinant HF wavefunctions for the supermolecule X and a monomer A. Using various approximate HF energy expressions for the supermolecule, the total HF interaction energy ΔE^{HF} can be decomposed into electrostatic, exchange, repulsion and polarization terms:

$$\Delta E^{HF} = \Delta E^{elec} + \Delta E^{ex} + \Delta E^{rep} + \Delta E^{pol} \quad (9)$$

Electrostatic interaction

The electrostatic interaction arises from the Coulomb's law, which considers the electrostatic interaction between two different charges. This means that the force of attraction or repulsion between two electrically charged bodies is direct interaction proportional to the strength of the electrical charges and inversely proportional to the square of the distance between them ^[8b].

$$V = \frac{Q_1 Q_2}{4\pi\epsilon_0 r} \quad (10)$$

Where Q1 and Q2 are the partial charges, r is their separation and ϵ_0 is the vacuum permittivity.

In this work, the electrostatic interaction is defined as

$$E^{elec} = \sum_a 2(a|\hat{V}_B|a) + \sum_b 2(b|\hat{V}_A|b) + \sum_{a,b} 4(aa|bb) + V_{AB} \quad (11)$$

Polarization energy

This energy arises from the distortion of a particular molecule in the electric field of all its neighbours and is always attractive. Because the fields of several neighbouring molecules may reinforce each other or cancel out, polarization is always non-additive.

The polarization energy is defined as

$$\Delta E^{pol} = E_X^{HF} - E_X^{(3)} \quad (12)$$

Where E_X^{HF} is the HF energy of the supermolecule X and $E_X^{(3)}$ is the energy expectation value of the system with the unrelaxed (and generally non-orthogonal) orbitals of the two individual subsystems which can be evaluated as

$$\begin{aligned}
E_X^{(3)} &= \sum_{i \in X}^{\alpha, \beta} \sum_{j \in X}^{\alpha, \beta} h_{ij} (S^{-1})_{ij} + \frac{1}{2} \sum_{i \in X}^{\alpha, \beta} \sum_{j \in X}^{\alpha, \beta} \sum_{k \in X}^{\alpha, \beta} \sum_{l \in X}^{\alpha, \beta} \langle ij|kj \rangle \\
&\times (S^{-1})_{ij} \times (S^{-1})_{kl} - \frac{1}{2} \sum_{i \in X}^{\alpha} \sum_{j \in X}^{\alpha} \sum_{k \in X}^{\alpha} \sum_{l \in X}^{\alpha} \langle ij|kj \rangle \\
&\times (S^{-1})_{ij} \times (S^{-1})_{kl} - \frac{1}{2} \sum_{i \in X}^{\beta} \sum_{j \in X}^{\beta} \sum_{k \in X}^{\beta} \sum_{l \in X}^{\beta} \langle ij|kj \rangle \\
&\times (S^{-1})_{ij} \times (S^{-1})_{kl} + E_X^{nuc}
\end{aligned} \tag{13}$$

Where i, j, k, and l are the orthonormal HF spin orbitals of the monomers and are not necessarily orthonormal to each other between the monomers; S^{-1} is the inverse of the overlap matrix S of all of the monomer spin orbitals.

3.5.2 Kohn-Sham method

The Kohn-Sham density functional interaction ΔE^{KS} can be decomposed into electrostatic, exchange, repulsion, polarization and dispersion terms

$$\Delta E^{KS} = \Delta E^{elec} + \Delta E^{ex} + \Delta E^{rep} + \Delta E^{pol} + \Delta E^{disp} \tag{14}$$

Electrostatic interaction

The KS electrostatic interaction energy is defined in eq. (11)

Polarization energy

The KS polarization energy is defined as

$$\Delta E^{pol} = E_X^{(4)} - E_X^{(3)} \tag{15}$$

Where $E_X^{(4)}$ and $E_X^{(3)}$ are written as

$$\begin{aligned}
E_X^{(3)} &= \sum_{i \in X}^{\alpha, \beta} \sum_{j \in X}^{\alpha, \beta} h_{ij} (S^{-1})_{ij} + \sum_{i \in X}^{\alpha, \beta} \sum_{j \in X}^{\alpha, \beta} \sum_{k \in X}^{\alpha, \beta} \sum_{l \in X}^{\alpha, \beta} \langle ij|kj \rangle \times (S^{-1})_{ij} (S^{-1})_{kj} \\
&+ E_X [\rho_X^{\alpha*}, \rho_X^{\beta*}] + \sum_A E_c [\rho_A^\alpha, \rho_A^\beta]
\end{aligned} \tag{16}$$

$$\begin{aligned}
E_X^{(4)} &= \sum_{i \in X}^{\alpha, \beta} \sum_{i \in X}^{\alpha, \beta} + \frac{1}{2} \sum_{i \in X}^{\alpha, \beta} \sum_{j \in X}^{\alpha, \beta} \sum_{k \in X}^{\alpha, \beta} \sum_{l \in X}^{\alpha, \beta} \langle ij|kj \rangle \times (S^{-1})_{ij} (S^{-1})_{kj} \\
&+ E_X [\rho_X^\alpha, \rho_X^\beta] + \sum_A E_c [\rho_A^\alpha, \rho_A^\beta] + E_X^{nuc}
\end{aligned} \tag{17}$$

Where i, j, k, and l are the variationally determined KS spin orbitals for the monomers and are not necessarily orthonormal to each other between the monomers; S^{-1} is not a unit matrix. The $\rho_X^{\alpha*}$ and $\rho_X^{\beta*}$ in eq. (16) are the alpha-spin and beta-spin electron density functions calculated using the orthonormalized monomer KS spin orbitals. ρ_X^α and ρ_X^β are the supermolecular electron densities that minimize the KS energy of the supermolecule and ρ_A^α and ρ_A^β are the monomer electron density functions that minimize the KS energy of each monomer.

Dispersion energy

Dispersion is an effect that cannot easily be understood in classical terms, but it arises because the charge distributions of the molecules are constantly fluctuating as the electrons move. The motions of electrons in the two molecules become correlated, in such a way that lower-energy configurations are favoured and higher-energy ones disfavoured. The average effect is a lowering of the energy, and since the correlation effect becomes stronger as the molecules approach each other, the result is an attraction.

$$\Delta E^{disp} = E_c [\rho_X^\alpha, \rho_X^\beta] - \sum_A E_c [\rho_A^\alpha, \rho_A^\beta] \quad (18)$$

The exchange-repulsion energy is described in the previous point and the polarization energy is defined as the “orbital relaxation energy”.

5. E_{exr} calculation in N_2 -He and Cl_2 -He systems

5.1 Computational details

All calculations were carried out using a shell script “exr-approx.chr” which employs Hartree-Fock method. Different basis sets were used here in order to study the validity of each to the system, mainly TZVP, cc-pVTZ, cc-pVDZ, and aug-cc-pVDZ.

In this script, the distance between both monomers, the basis set and the orbitals of interest were chosen to carry out the E_{exr} calculation.

5.2 N_2 -He System

This system consists of a N_2 molecule and a He atom. The aim is to study the exchange-repulsion interaction of the He 1s orbital with the seven molecular orbitals of the N_2 molecule in the directions x and y (shown in the next section).

5.2.1 Description of the system

The N_2 molecule is fixed with its centre in the origin of the coordinate system and the N atoms on the z-axis. The real bond distance of the N_2 (0.548844 Å) is taken from the NIST data base ^[8].

First, the He atom is positioned on the origin of the coordinate system. Then, it is shifted by steps of 0.2 Å along the x-axis and y-axis. The final position in both cases is 7.0 Å from the origin of the coordinate system. Figure 1 shows the initial and final position of the system.

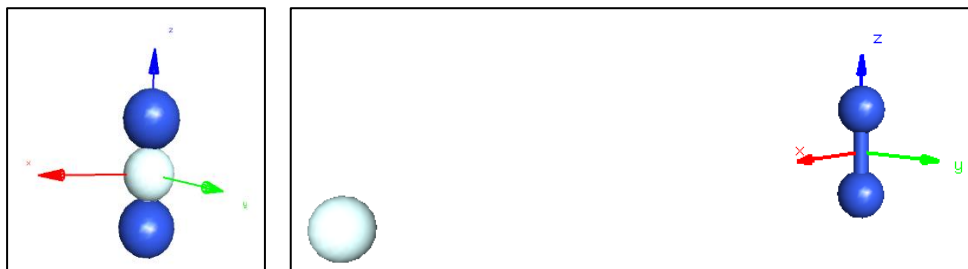


Figure 1: Left: initial position. Right: final position when the He is on the x-axis. The final position when the He is on the y-axis is the same as the photo on the right but on the y-axis.

5.2.2 Orbitals studied

We investigated how the seven occupied molecular orbitals of the N_2 molecule contribute to E_{ext} with the He 1s orbital. All orbitals are represented in figures 2 and 3.

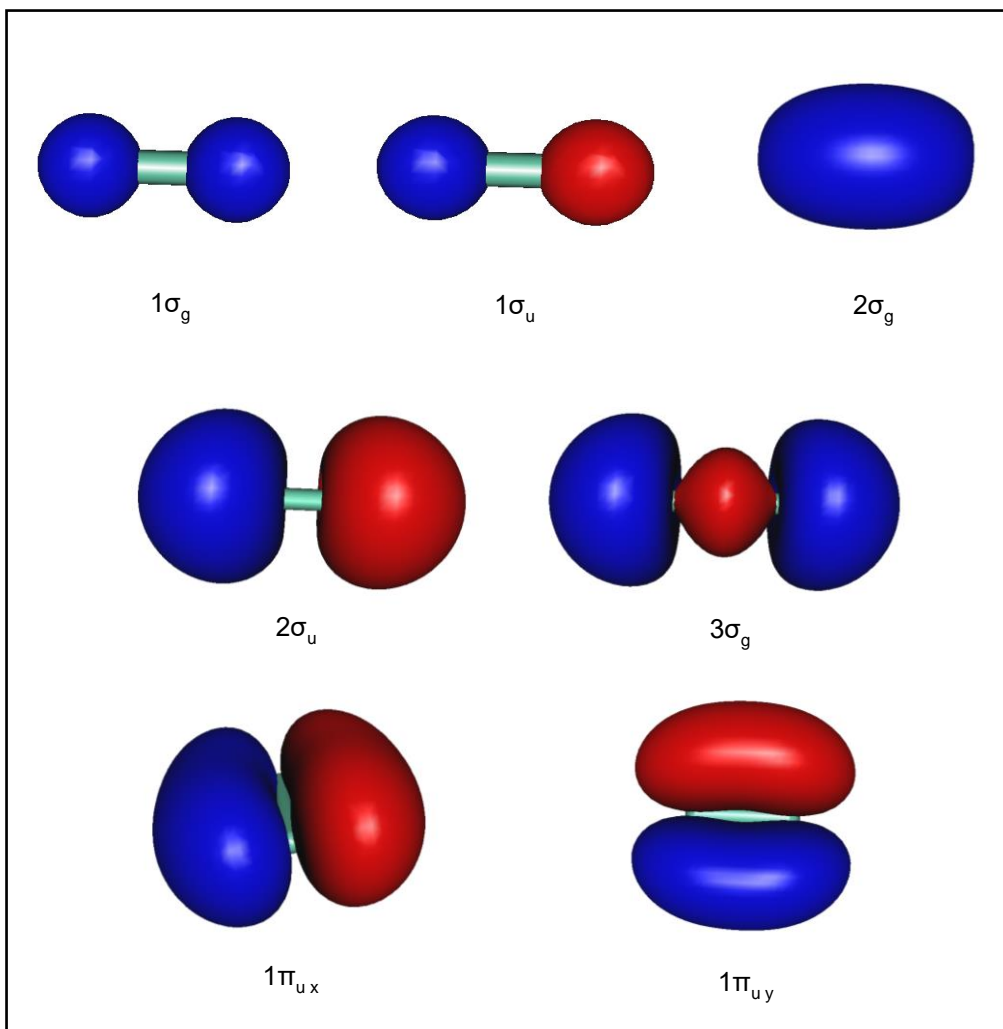


Figure 2: Seven molecular orbitals of N_2 .

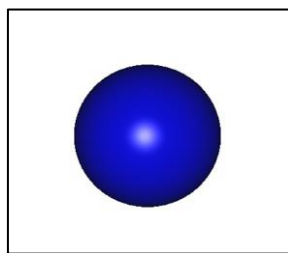


Figure 3: 1s He orbital.

5.2.3 Basis sets quality

Figure 4 shows the behaviour of different basis sets used when the He atom was shifted along the x-axis.

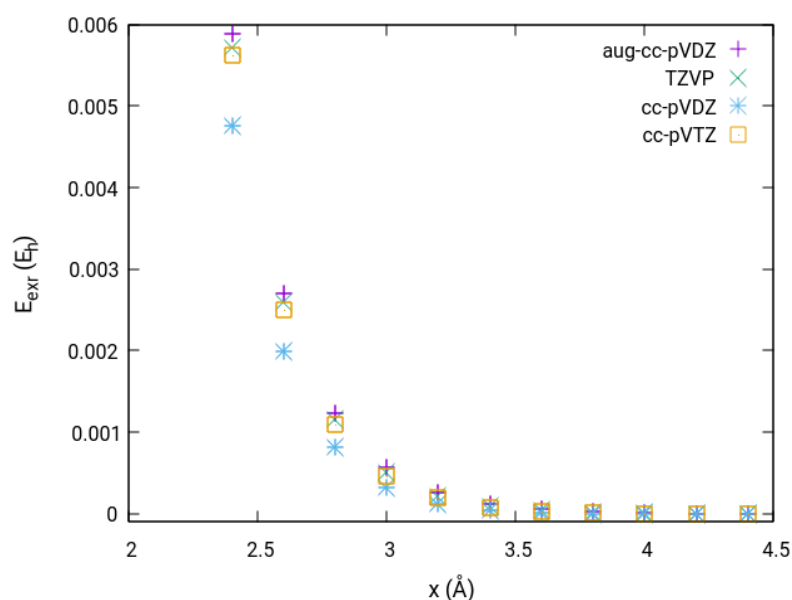


Figure 4: N₂-He, representation of basis sets behaviour when He is shifted on the x-axis.

As explained earlier, the type of basis functions used are GTO's, and the r^2 dependence in the exponential (eq. 1 and 2) makes the GTOs falling off too rapidly far from the nucleus. But, depending on the number of basis functions used, the quality of representation will be affected.

Here, the poorest representation is provided by the cc-pVDZ basis set. In this basis set each valence orbital is represented by two basis functions. As the TZVP and cc-pVTZ basis sets contain one more function, they allow for a better quality representation of the orbitals and, thus of the exchange repulsion energy.

The basis set which provides a better quality representation is aug-cc-Pvdz. This can be explained by the presence of diffuse functions: one extra function for each angular momentum is added.

The basis set behaviour when the He atom was shifted along the y-axis is the same (see appendix). Therefore, the basis set chosen to show the results obtained is aug-cc-pVDZ.

5.2.4 Results and discussion

5.2.4.1 Orbitals which contribute most to the E_{extr}

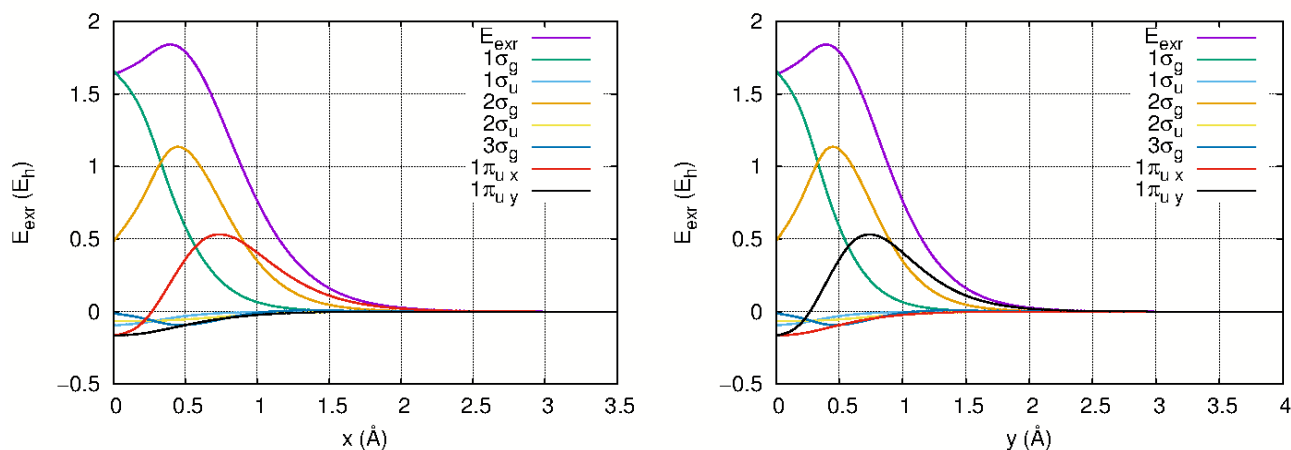


Figure 5: Representation of E_{extr} (E_h) vs distance (\AA). Left: He is shifted along the x-axis. Right: He is shifted along the y-axis.

Figure 5 shows all the energy contributions of the interaction between the seven molecular orbitals of the N_2 and the orbital of the He atom in x and y displacements. The curves are designated according to the names of the contributing orbitals N_2 orbitals.

E_{extr} is not always larger in absolute value than the repulsion energy. For instance, the E_{extr} is negative when $x=0 \text{ \AA}$ and $y=0 \text{ \AA}$ (figure 5) in the representation of the $1\pi_{ux}$ and $1\pi_{uy}$ orbital, respectively. This is due to the vanishing overlap of the He 1s with $\text{N}_2 \pi_{ux}$ and 1s with $\text{N}_2 \pi_{uy}$.

When He is shifted along the x-axis, the orbitals which contribute most to the E_{extr} are $2\sigma_g$ and $1\pi_{ux}$.

Orbital $2\sigma_g$ has a bump when $x=0.5 \text{ \AA}$ and orbital $1\pi_{ux}$ when $x=0.75$. This is due to the overlap of $2\sigma_g$ and $1\pi_{ux}$ with the He 1s orbital caused by the symmetry of the system. In both cases, there are two mirror planes and one C_2 axis.

Table 1. E_{extr} values at different positions

x value (\AA)	$2\sigma_g(E_h)$	$1\pi_{ux}(E_h)$
0.4	1.12	-
0.8	-	0.52

In both cases, it has not any physical sense as long as it is impossible to put both monomers together. The E_{extr} at these points is extremely large as it can be seen in Table 1. In the hypothetical case that this was possible, the triple bond between the two nitrogen atoms will be broken and both atoms will be extremely separated.

Calculations allow us to confirm that the origin of the E_{exr} is caused by the overlap between both systems.

It is also possible to observe that $1\sigma_g$ also contributes when $x=0 \text{ \AA}$. However, in reality, He atom cannot be placed in the middle of the N_2 molecule. For this reason, the discussion of its contribution is skipped in this part.

The distances where there is not exchange repulsion are represented in figure 6. This is explained in more details in the next section.

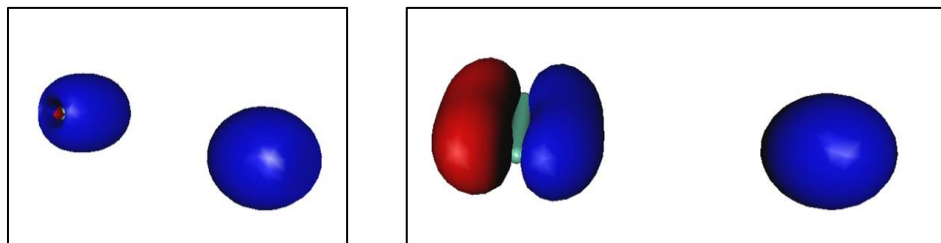


Figure 6: Left: $2\sigma_g$ with the He 1s orbital when $x=4.0 \text{ \AA}$. Right: $1\pi_{ux}$ with the He 1s orbital when $x=4.0 \text{ \AA}$.

When He is shifted along the y -axis the orbitals which contribute most to the E_{exr} are not exactly the same as in figure 6. In this case, the orbitals are $2\sigma_g$ and $1\pi_{uy}$.

Orbital $2\sigma_g$ has a bump when $x=0.5 \text{ \AA}$ and orbital $1\pi_{uy}$ when $y=0.7 \text{ \AA}$. The reason of both bumps is the same as in the previous case. The E_{exr} of $1\pi_{uy}$ when $y=0.75 \text{ \AA}$ is the same as in the previous case when $x=0.75 \text{ \AA}$ (Table 1) due to the same symmetry.

The following picture shows $1\pi_{uy}$ orbital at an appropriate distance. This is justified in the next section (optimal distance).

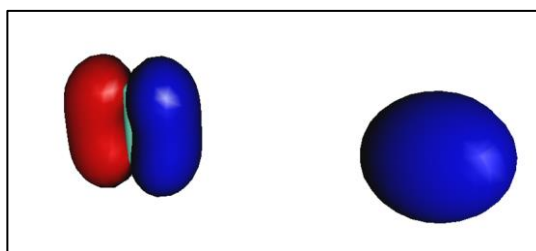


Figure 7: $1\pi_{uy}$ of N_2 with the He 1s orbital when $y=4.0 \text{ \AA}$.

5.2.4.2 Optimal distance

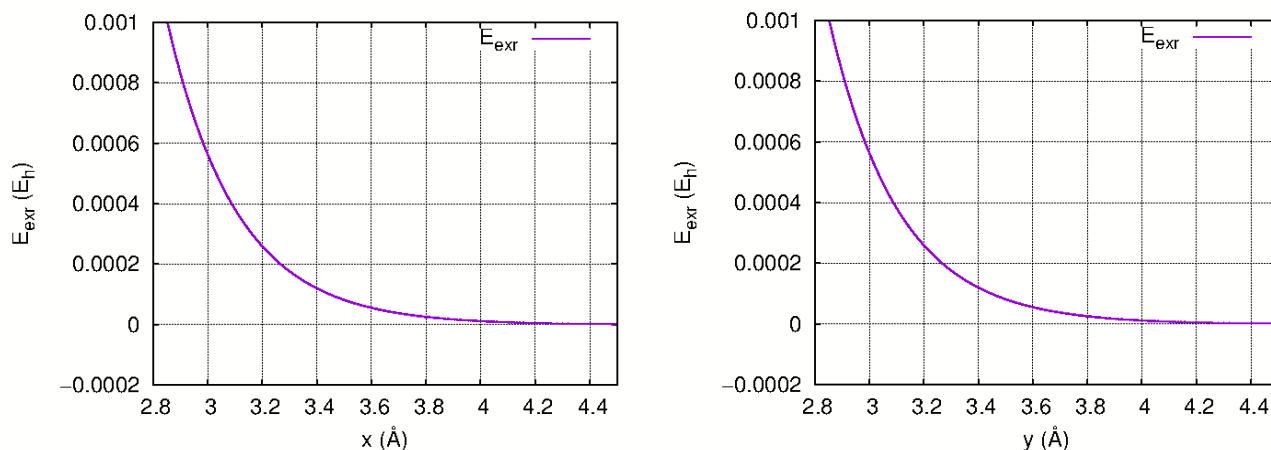


Figure 8: Zoom of E_{exr} in Figure 2. Left: He is shifted along the x-axis. Right: He is shifted along the y-axis.

In figure 8, E_{exr} is shown for more realistic distances between both monomers in which the E_{exr} is less than about $0.001 E_h \approx 2.6 \text{ kJ/mol}$. Approximately when x and $y=4 \text{ Å}$ the E_{exr} becomes very small ($6.26 \cdot 10^{-8} E_h$). In both cases, the E_{exr} value is the same because both structures are equivalent by symmetry. It can be concluded that when N_2 and He are in a distance longer than 4 Å E_{exr} becomes negligibly small.

5.3 Cl_2 -He System

This system consists of Cl_2 molecule and He atom. As in the N_2 -He case, the exchange-repulsion interaction of the He 1s orbital with the last seven molecular orbitals of Cl_2 is analysed in the x and y directions.

5.3.1 Description of the system

Same as N_2 -He system. The real bond distance (0.99395 Å) of the Cl_2 is taken from the NIST page ^[9].

The system studied is illustrated in figure 9. The initial and final positions are the same as in the N_2 -He system.

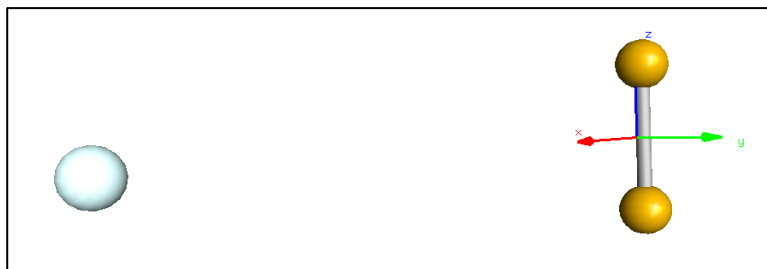


Figure 9: Example of Cl_2 -He system when $x=7.0 \text{ Å}$.

5.3.2 Orbitals studied

The seven molecular orbitals of the Cl_2 interacting with the He 1s orbital are represented in figure 10.

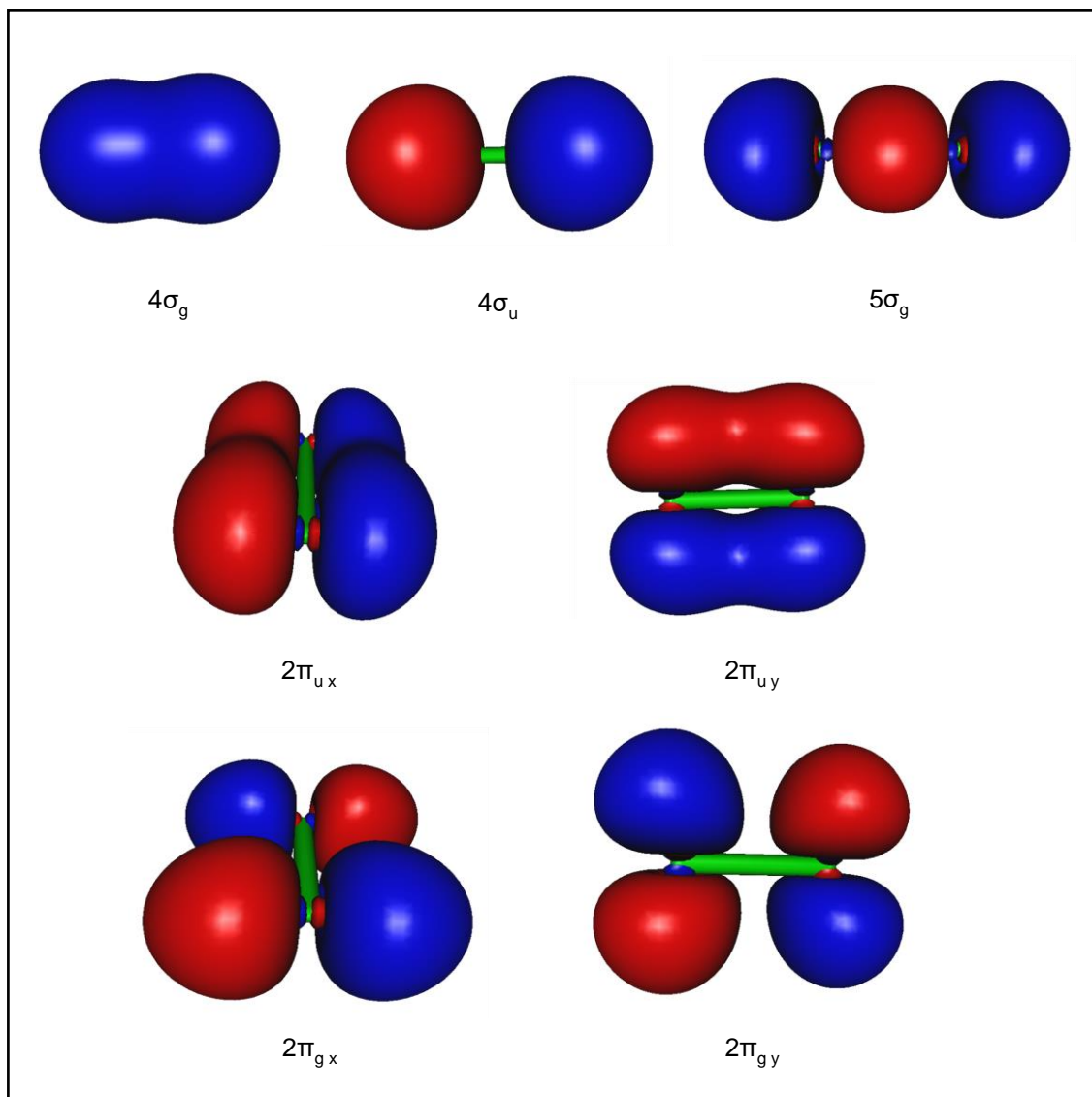


Figure 10: Seven molecular orbitals of Cl_2 .

5.3.3 Basis sets quality

Figure 11 shows the behaviour of the different basis sets used when the He atom was shifted along the x-axis.

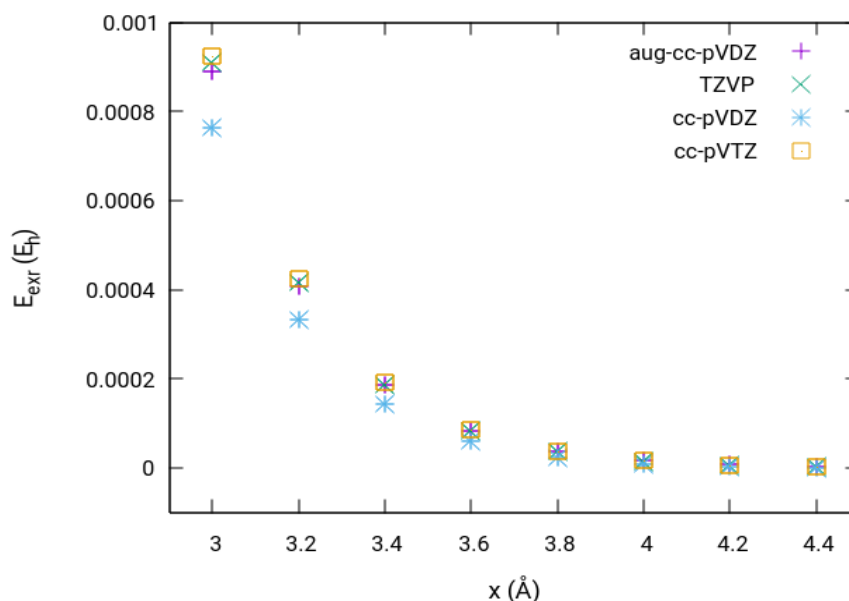


Figure 11: Cl₂-He, representation of basis sets behaviour when He is shifted on the x-axis.

Here, the poorest representation is provided by the cc-pVDZ basis set. In this basis set each valence orbital is represented by two basis functions. The following bases: aug-cc-pVDZ, TZVP and cc-pVTZ show a similar behaviour..

The basis set which provides a better quality representation is cc-pVTZ. This can be explained by the correlation consistent term and the triplication of the number of valence orbitals.

The basis set behaviour when the He atom was shifted along the y-axis is the same (see appendix). Therefore, the basis set chosen to show the results obtained is cc-pVTZ.

5.3.4. Results and discussion

5.3.4.1 Orbitals which contribute most to the E_{exr} .

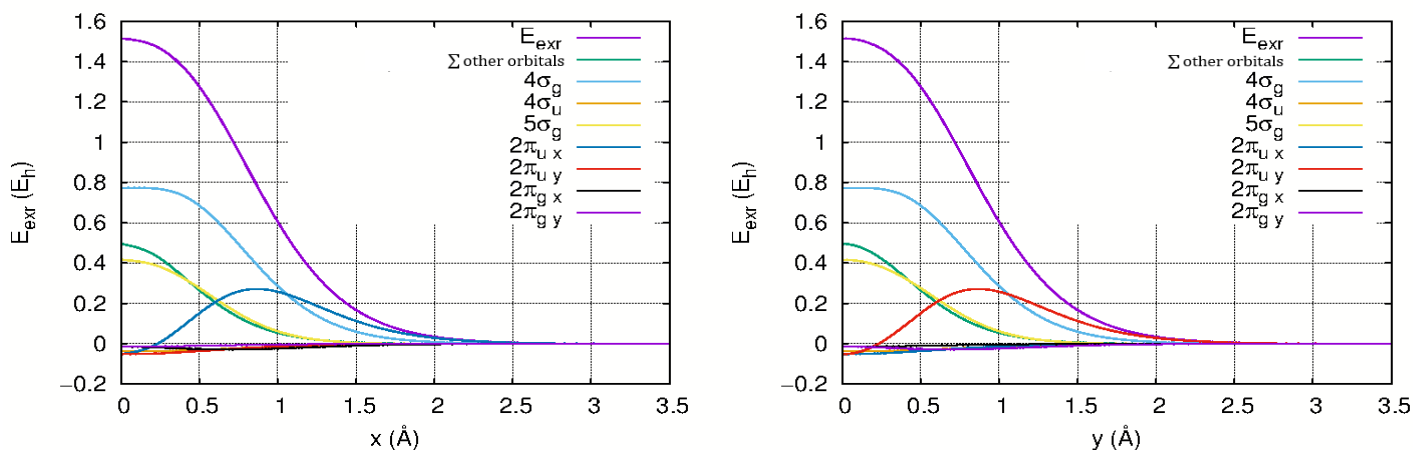


Figure 12: Representation of E_{exr} (E_h) vs distance (\AA). Left: He is shifted along the x-axis. Right: He is shifted along the y-axis.

In figure 12, it is possible to observe the energy contributions of the interaction between the last seven molecular orbitals of the Cl_2 and the orbital of the He atom. The curves are designed according to the names of the contributing Cl_2 orbitals.

The orbital contribution to E_{exr} is negative when $x=0 \text{ \AA}$ in the representation of the $4\sigma_u$, $2\pi_{u_x}$, $2\pi_{u_y}$, $2\pi_{g_x}$ and $2\pi_{g_y}$ orbitals. This is due to the vanishing overlap of the He $1s$ with the orbitals mentioned.

When He is shifted along the x-axis, the orbital which contributes most to the E_{exr} is $2\pi_{u_x}$. Its representation has a maximum when $x=0.8 \text{ \AA}$ because of the overlap of $2\pi_{u_x}$ and $1s$ He orbital at this distance as a result of system's symmetry. In this case too, there are two mirror planes and one C_2 axis as symmetry elements.

Again, arrangements with exchange repulsion energies above 0.1 mE_h have little physical meaning due to the impossibility of put both monomers at this position. The full exchange-repulsion energy is extremely large ($0.27 E_h$). In the hypothetical case that this was possible, the bond between both chlorine atoms will be broken and both atoms will be extremely separated.

In this case, HOMO ($2\pi_{g_x}$) and HOMO -1 ($2\pi_{g_y}$) do not overlap with the He $1s$ orbital in the considered geometry and their contribution to the exchange-repulsion energy is therefore small.

It is also possible to observe that electron core orbitals such $4\sigma_g$ and $5\sigma_g$ also contribute when $x=0 \text{ \AA}$. Their contribution is not commented because it does not make sense since He atom at this position is impossible and E_{exr} values are extremely large.

$2\pi_{u_x}$ of Cl_2 and $1s$ He orbitals at $x=4.2 \text{ \AA}$ are shown in figure 13.

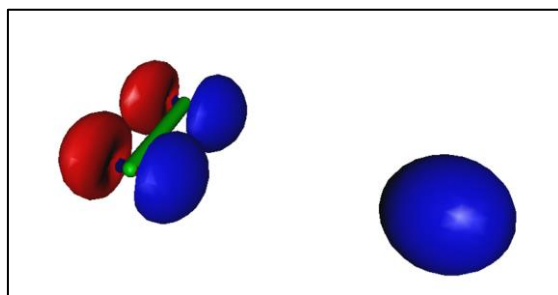


Figure 13: $2\pi_{ux}$ of Cl_2 with the He 1s orbital when $x=4.2 \text{ \AA}$.

When He is shifted along the y-axis, the orbitals which contribute most to the E_{exr} are not the same as in figure 13. In this case, the orbital contributing differently is $2\pi_{uy}$, which has a bump when $y=0.75 \text{ \AA}$. The reason of this bump is the same as in the previous case. The E_{exr} of $2\pi_{uy}$ when $y=0.75 \text{ \AA}$ is also the same as in the previous case when $x=0.75 \text{ \AA}$ because in both situations the symmetry is the same.

Figure 14 shows $2\pi_{uy}$ orbital at an appropriate distance from 1s of He.

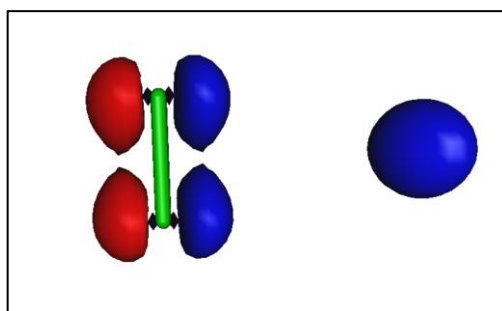


Figure 14: $2\pi_{uy}$ of Cl_2 with the He 1s orbital when $v=4.2 \text{ \AA}$.

5.3.4.2 Optimal distance

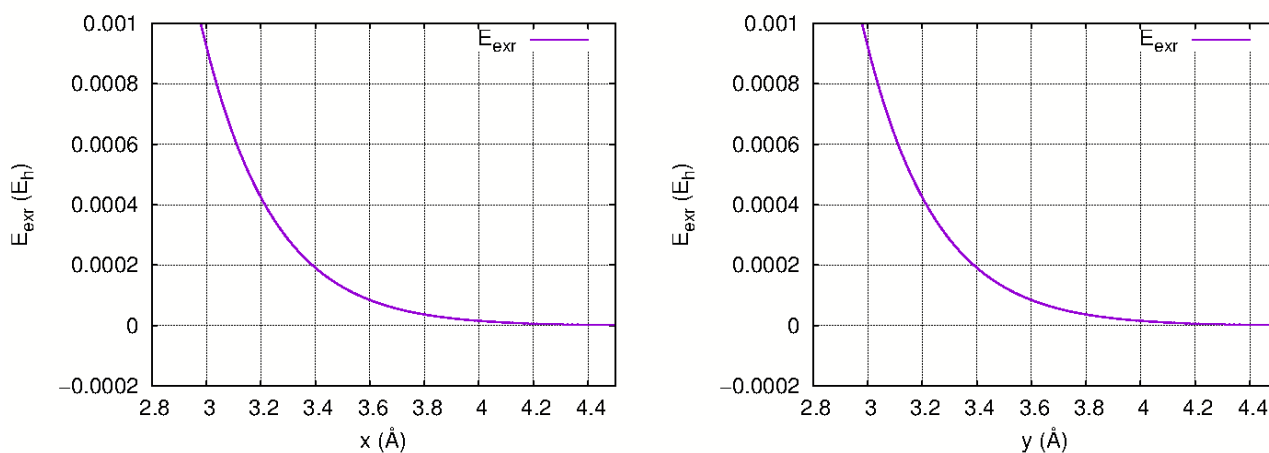


Figure 15: Zoom of E_{exr} in Figure 5. Left: He is shifted along the x-axis. Right: He is shifted along the y-axis.

In figure 15, it can be observed that approximately when x and $y=4.2 \text{ \AA}$, E_{extr} is null ($6.58 \cdot 10^{-6} E_h$). This distance corresponds to the optimal arrangement of both systems. It can be concluded that when Cl_2 and He are in a distance on the x and y -axis longer than 4.2 \AA there is not any interaction and there is no E_{extr} .

6. Energy decomposition analysis

The aim of this section consists in studying how all the total interaction energy is decomposed according to the EDA scheme explained in the theoretical part for the N_2 -He and Cl_2 -He systems.

6.1 Computational details.

These calculations were performed with TUBOMOLE using HF and DFT (B-LYP) methods. The basis set used are TZVP, cc-pVTZ, cc-pVDZ, and aug-cc-pVDZ.

The energies shown in eq. (9) were calculated.

6.2 N_2 -He

6.2.1 Description of the system

The N_2 molecule is fixed with its centre in the origin of the coordinate system and the N atoms on the z -axis whole.

First, the He atom is positioned 3.4 \AA from the origin of coordinates on the z -axis. Then, it is shifted by steps of 0.4 \AA along the x -axis, y -axis, and z -axis. In the last case, the initial position of the He atom is $z=3.0 \text{ \AA}$. The final position in all cases is 5.0 \AA from the origin of the coordinate system.

The following photos show the initial and final position of the system

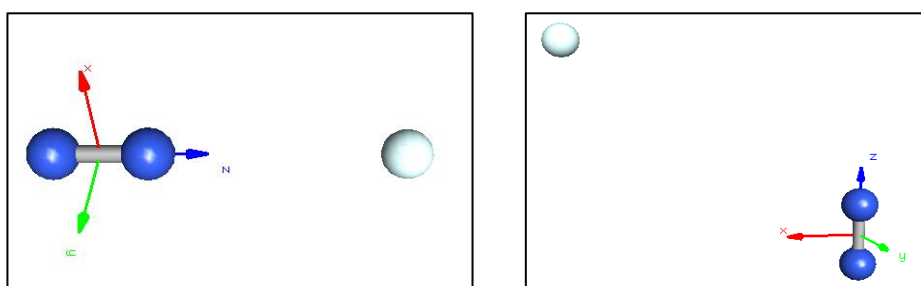


Figure 16: Right: initial position. Left: Final position when the He is on the x -axis. The final position when He is on the z -axis is the same as the photo on the right but at a longer distance. The final position when He is on the y -axis is the same as the photo on the right but in the y -axis.

6.2.2 Basis sets quality

The comparison between all basis sets in all displacements in both HF and B-LYP calculations show the same behaviour as in the exchange-repulsion calculation (see appendix). Therefore, the results shown in the next sections correspond to the calculations with the aug-cc-pVDZ as a basis set.

6.2.3 HF calculation

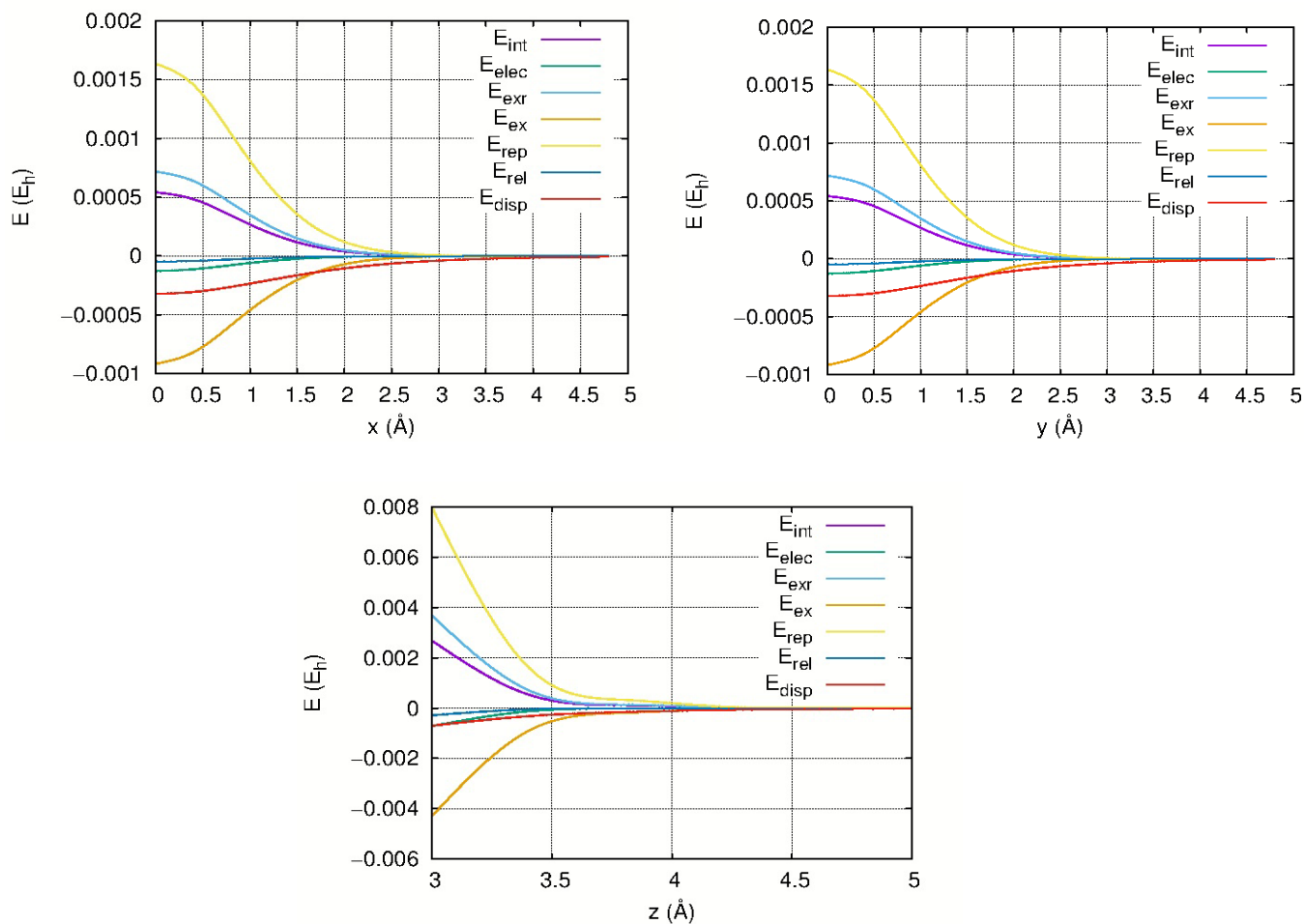


Figure 17: HF, aug-cc-pVDZ. EDA representation. Left: He shifted on the x-axis. Right: He shifted on the y-axis. Bottom: He shifted on the z-axis.

In all cases, it is possible to observe that the E_{exr} is the one which contributes most to the total E_{int} . Although in EDA there is no E_{disp} , it is also possible to calculate it. This is because an empirical correction which works similar to force fields calculation has been calculated. This empirical correction is called dispersion correction D3(BJ).

6.2.4 DFT calculation

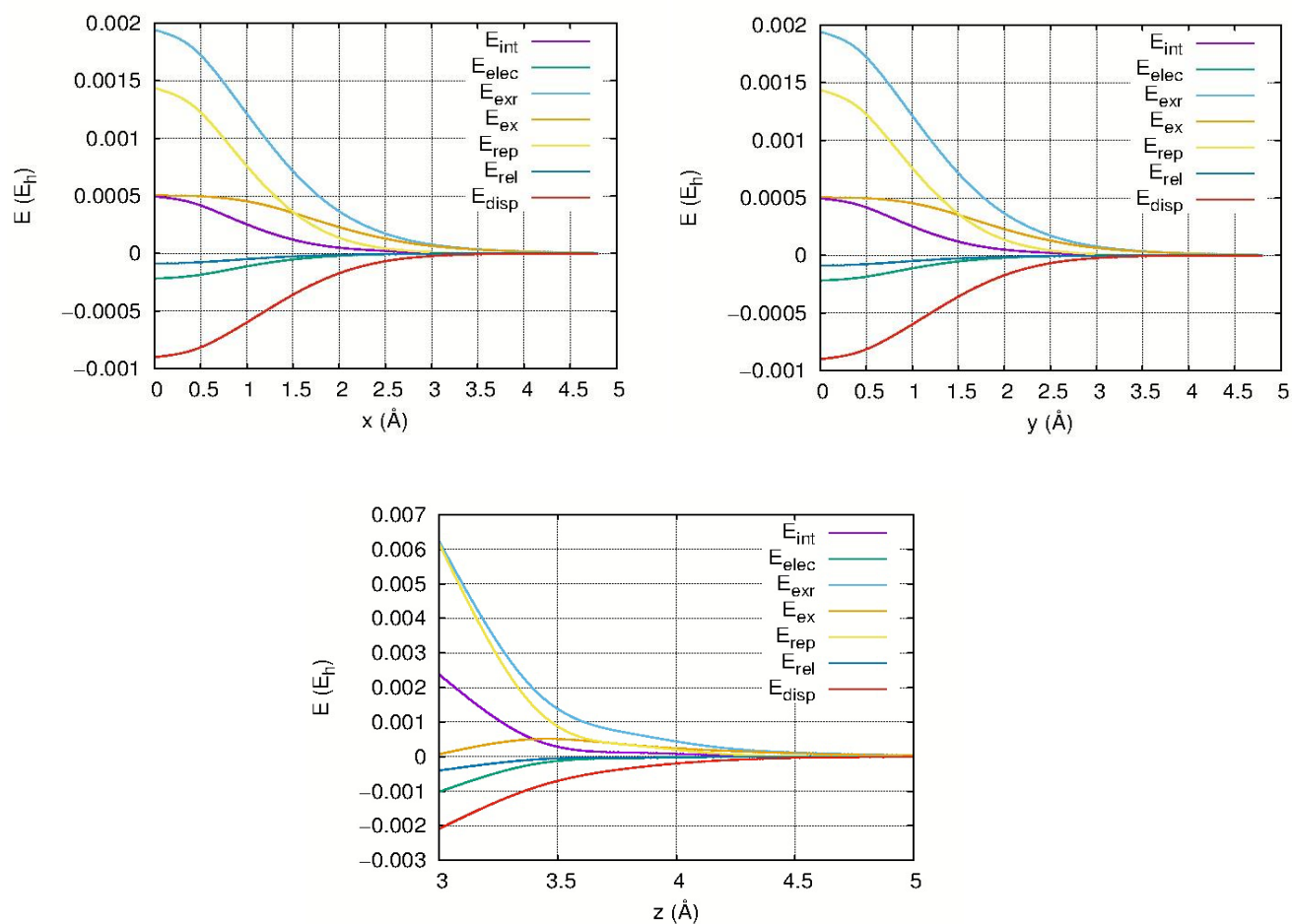


Figure 18: B-LYP, aug-cc-pVDZ. EDA representation. Left: He shifted on the x-axis. Right: He shifted on the y-axis. Bottom: He shifted on the z-axis.

In all cases, it is also possible to observe that the E_{exr} is the one who contributes most to the total E_{int} . The difference between HF and DFT calculation is that E_{ex} in the last case is positive, which differs from its own definition. DFT allows to calculate it since it considers that the total energy of the dimer is less negative than the one of each individual monomer.

6.3 Cl₂-He

6.3.1 Description of the system

It is the same situation as in the N₂-He system. The following figure shows the system studied. The initial and final positions are the same as in the N₂-He system.

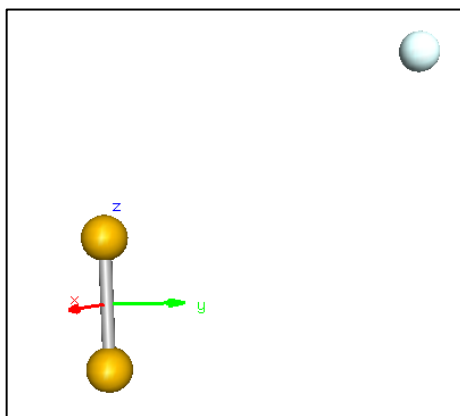


Figure 19: Example of Cl₂-He system when the He is on the x-axis.

6.3.2 HF calculation

6.3.2.1 Basis sets quality

The comparison between all basis sets in all displacements shows the same behaviour as in the exchange-repulsion calculation (see appendix). Therefore, the corresponding results refer to the calculations with cc-pVTZ as a basis set.

6.3.2.2 Results

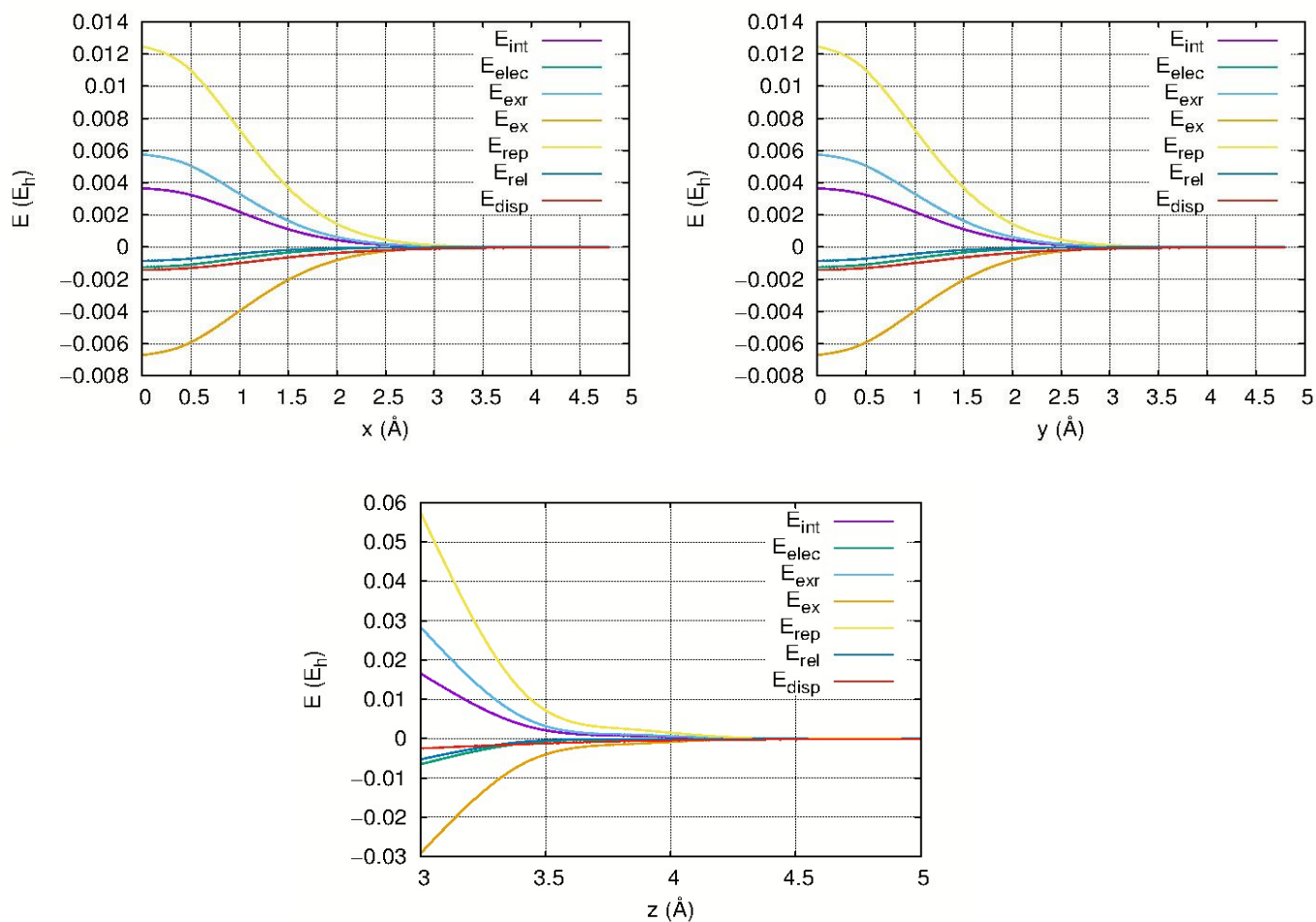


Figure 20. HF, cc-pVTZ. EDA representation. Left: He shifted on the x-axis. Right: He shifted on the y-axis. Bottom: He shifted on the z-axis.

In all cases, it is possible to observe that the E_{exr} is the one which contributes most to the total E_{int} . Again, E_{disp} can be observed although it does not appear in eq. 9 because it is obtained as an empirical correction which works similar to force field implementations. This empirical correction is called dispersion correction D3(BJ).

6.3.3 DFT calculation

6.3.3.1 Basis sets quality

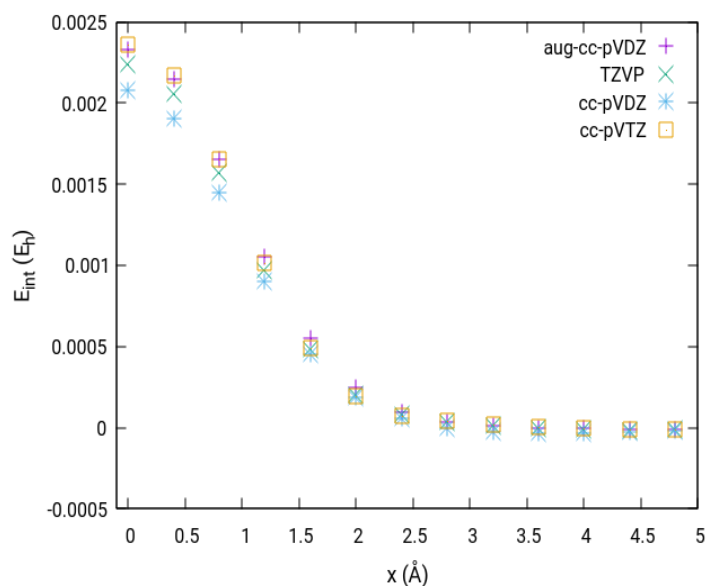


Figure 21: Cl₂-He B-LYP, EDA representation of basis sets behaviour when He is shifted on the x-axis.

When aug-cc-pVDZ is used as basis set, the E_{int} representation does not fall as rapid as the other ones.

The same behaviour is observed when He atom is shifted along y and z-axis (see appendix). Therefore, the results shown below correspond to the calculations with aug-cc-pVDZ as a basis set.

6.3.3.2 Results

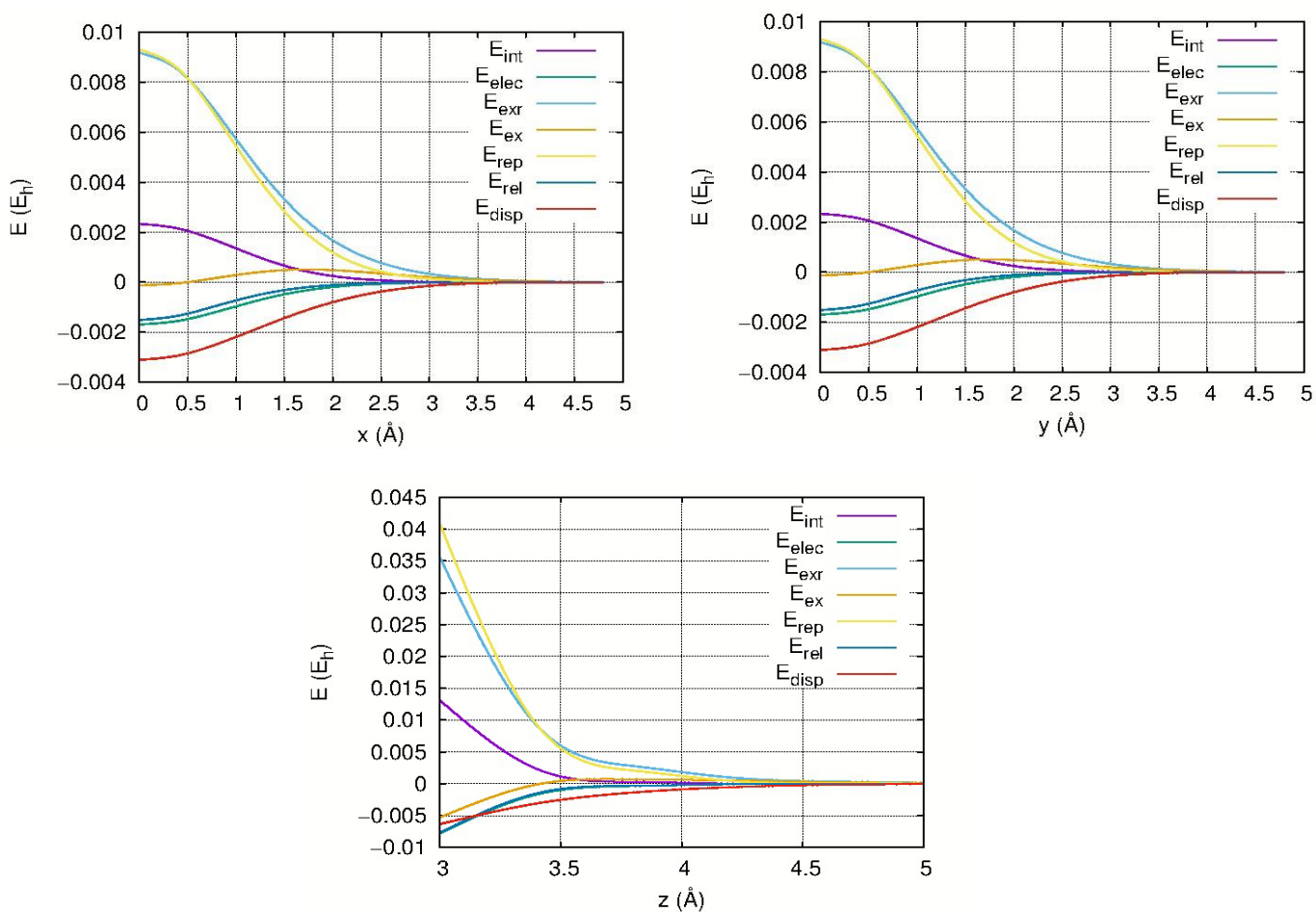


Figure 22: B-LYP, aug-cc-pVDZ. EDA representation. Left: He shifted on the x-axis. Right: He shifted on the y-axis. Bottom: He shifted on the z-axis.

Again, it is possible to observe that E_{exr} contributes most to the total interaction energy. The difference between HF and DFT calculation is that E_{ex} in the last case is positive, which differs from its own definition. The reason is the same as in the EDA B-LYP calculation in the N_2 -He system.

7. 2D Calculation

The aim of this section is to calculate E_{exr} in a 2D plane (xz) for $\text{N}_2\text{-He}$ and $\text{Cl}_2\text{-He}$ systems.

7.2. Computational details

The calculations were made with a personal script “exr-approx.csh” which uses HF method. The calculations were carried out with TZVP as a basis set. In this script, the distances between both monomers, the basis set and the orbitals of interest were chosen to carry out the 2D E_{exr} calculation.

7.3. $\text{N}_2\text{-He}$

7.3.1 Description of the system

The initial position of the system is the same as in figure 1. The difference here is that the calculations were made on the xz plane. The starter coordinates of the He was (0,0,0) Å and the final ones (5,0,5) Å. The He atom was also shifted by steps of 0.2 Å.

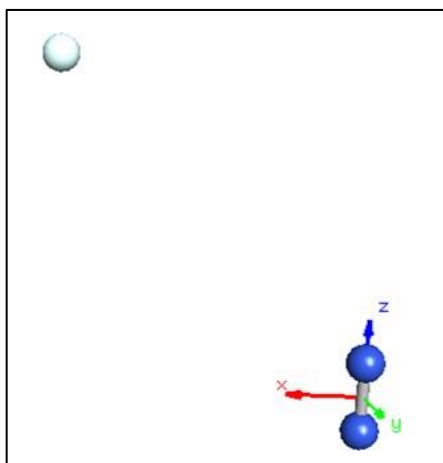


Figure 23: Final position of the He atom.

7.3.2 Results

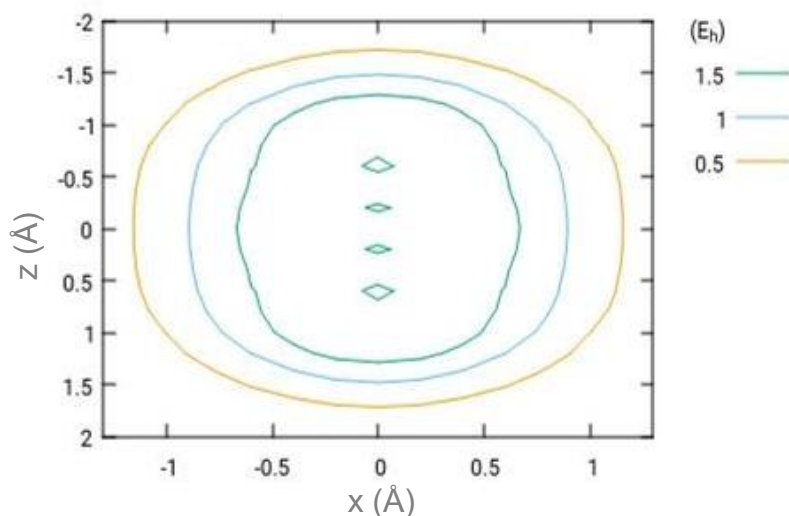


Figure 24: $\text{N}_2\text{-He}$ system. 2D (xz) plot of the E_{exr} isocontours.

In the previous plot, it is possible to observe isocontours which correspond to the same E_{exr} values. The lines with the same colour refer to positions having the same E_{exr} value. This is due to the same symmetry in these positions.

As it can be seen, the closer the two systems are, the greater the total E_{exr} value.

7.4 $\text{Cl}_2\text{-He}$

7.4.1 Description of the system

It is the same situation as in the previous case.

7.4.2 Results

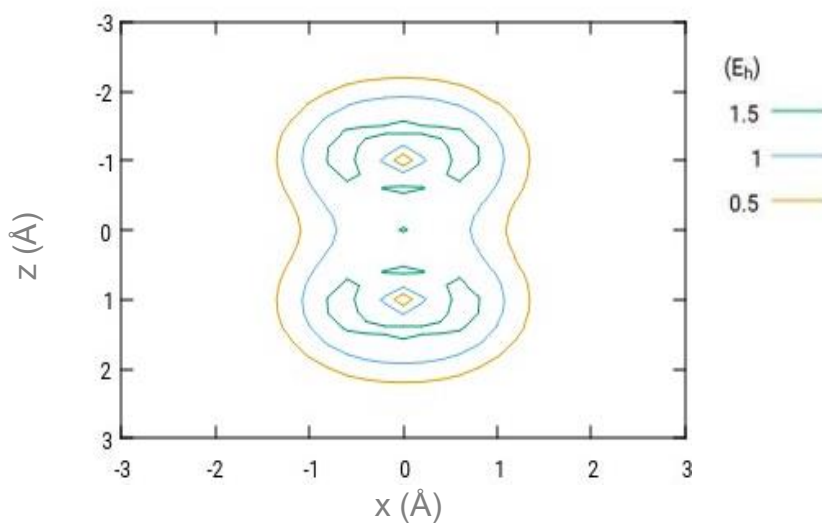


Figure 25: $\text{Cl}_2\text{-He}$ system. 2D (xz) plot of the E_{exr} isocontours.

In figure 25, the isocontours belong to positions which have the same symmetry.

Comparing figure 24 and 25, some differences can be observed. In figure 24 the shape along $x=0$ and $z=0$ Å is not as pronounced as in figure 25. This is due to the binding bond character of each diatomic molecule. N_2 has a triple bond and when He is closer to that bond there will be more E_{exr} than when it is closer to Cl_2 , which has a simple bond.

8. Introduction to Perylene Bisimides

According to the work of Steffan Grimme ^[9], the magnitude of the intermolecular interactions is more strongly size-dependent in aromatic systems than in saturated systems.

It was also concluded that the strongest interactions for stacked aromatic dimers become very significant for more than 10-15 carbon atoms. It is the binding mode and not only the presence of π electrons that determine the character of the interaction. Also, the electrostatic effects in the π - π stacked arrangements are minimized by parallel displacement, and the Pauli exchange repulsion becomes smaller when few filled orbitals overlap. Therefore, π - π stacking interactions really exist.

Thus, π - π stacking interactions can be used as a geometrical descriptor of the interaction mode in unsaturated molecules. Furthermore, these interactions should be understood as a special type of electron correlation effect that can only act in large unsaturated systems when they are spatially close, which is only possible in the stacked orientation.

In this work, interactions between two molecules of PBI have been studied.

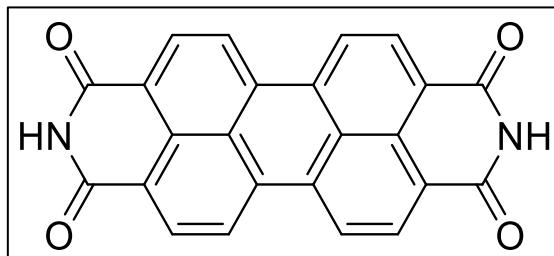


Illustration 2: Planar perylene bisimide (PBI) studied in this work.

Perylene bisimides have been used for decades as organic pigments, but currently, they are being investigated on other utilities, since they are one of the π -conjugated functional molecules with properties of great interest such as resistance to light, intense photoluminescence and properties of organic solar cells, organic transistors, diodes, and other electronic devices. The energy transport properties of these molecules are strongly dependent on the intermolecular interactions and the arrangement of the monomers in the material. Therefore, a design of its applications needs detailed knowledge about how geometric orientation of the molecules in these properties ^{[10],[11]}.

8.1 Description of the system

One PBI molecule (PBI1) is fixed with its center in the origin of the coordinate system with the long (longitudinal) axis of the molecule printed along the z-axis and the short (transversal) axis in y direction. The other PBI molecule (PBI2) is shifted by 3.4 Å along the x-axis above PBI1. Then PBI2 is shifted up to 10.0 Å along the z-axis. The same is made on the y-axis (see figure 26).

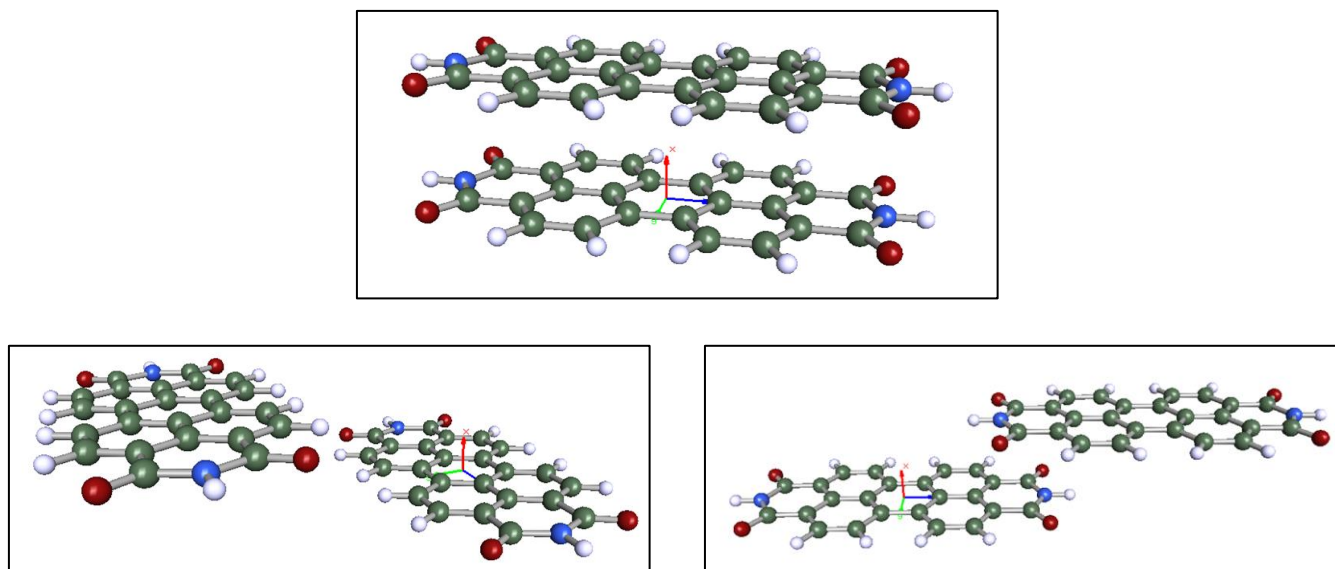


Figure 26: Top:Initial position. Left: PBI2 shifted along the y-axis. Right: PBI2 shifted along the z-axis

8.2 Computational details

The calculations were made with the same script as in the two first systems. The calculations were carried out with the TZVP basis set.

8.3 Orbitals studied

One molecule of PBI has 100 molecular orbitals. In this work, 16 π molecular orbitals have been studied and they are shown below in figure 27.

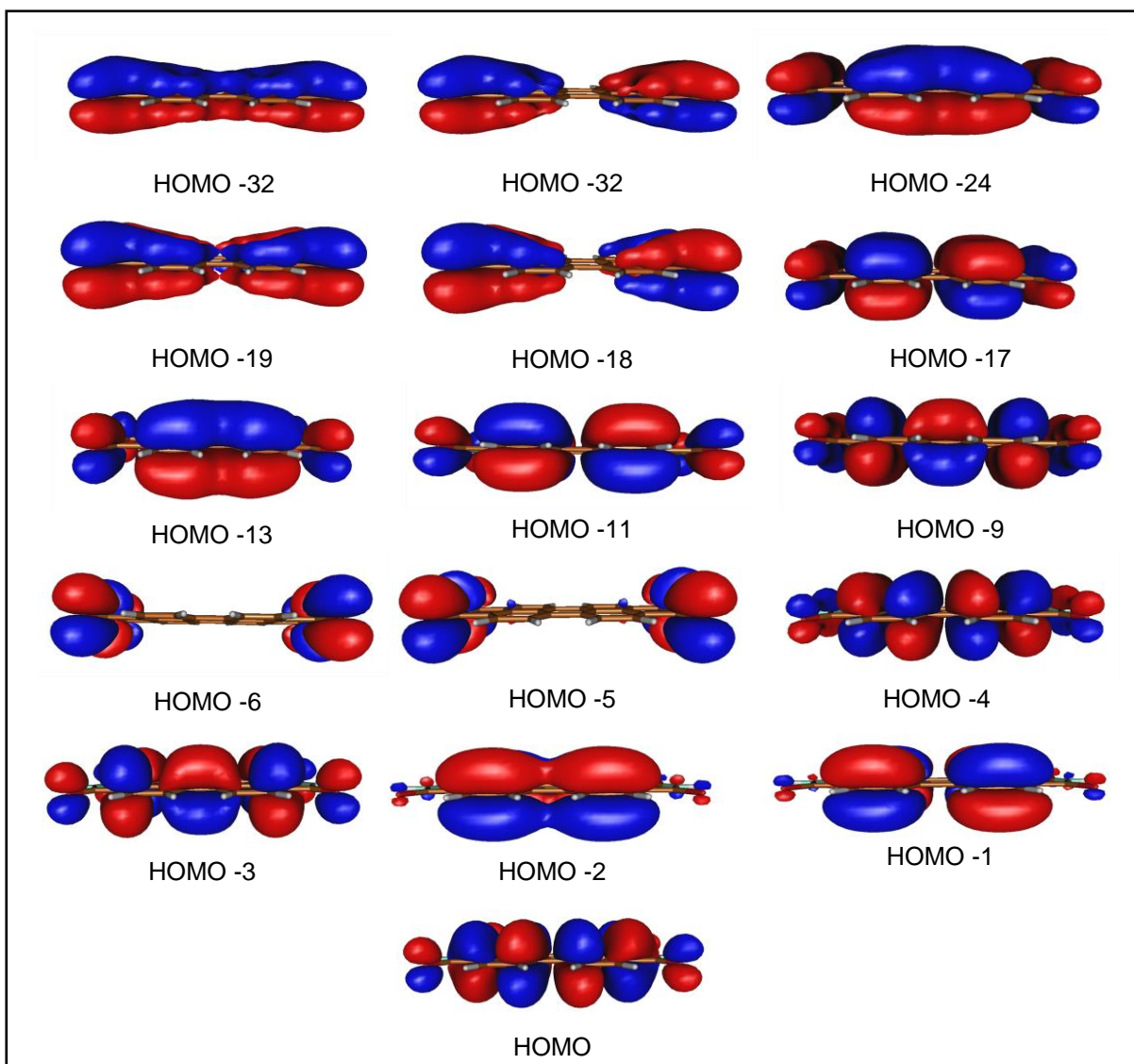


Figure 27: the PBI 16 π molecular orbitals studied.

8.4 Results when PBI2 is shifted along the z-axis

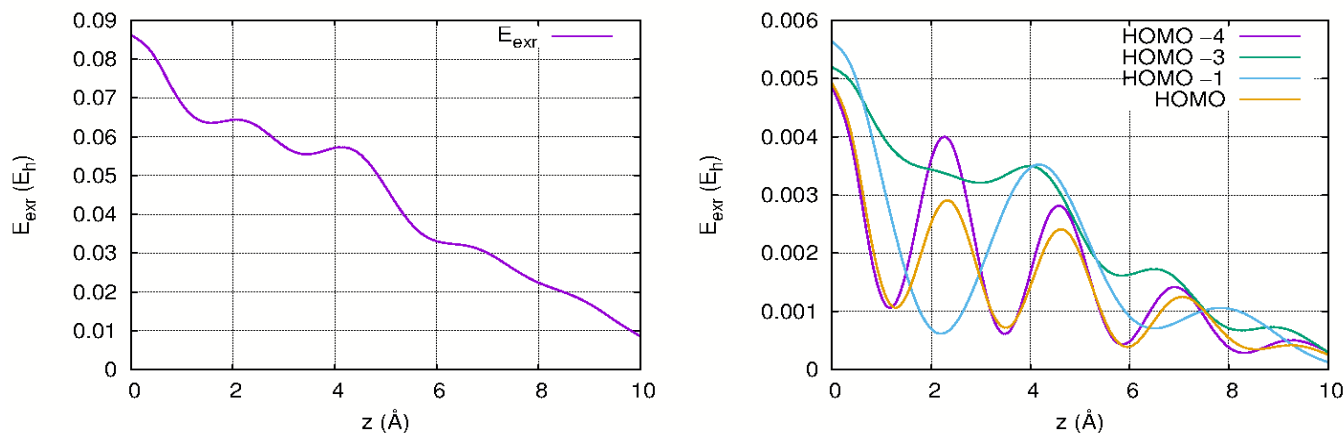


Figure 28: Left: representation of $E_{\text{exr}} (E_h)$ vs distance (\AA) when PB2 is shifted along the z axis. Right: orbitals which contribute most to the E_{exr} when PB2 is shifted along the z axis.

The left graphic in figure 28 shows four bumps when $z=2.4, 4.4, 6.8$ and 9.2 \AA .

HOMO orbital has 4 bumps and they can be observed when $z= 2.4, 4.4, 6.8$ and 9.2 \AA . This is due to the interaction between HOMO of PBI1 and PBI2. In these positions, both molecules interact and their orbitals overlap, this is possible due to the bonding or anti-bonding character of the orbitals. HOMO has 5 nodes. When HOMO of PBI2 is positioned on the nodes of PBI1, there is no interaction between both orbitals. The curves shown here indicate $E_{\text{exr}}(a) = \sum_b E_{\text{exr}}(a, b)$.

HOMO -4 representation shows the same behaviour as HOMO. HOMO -4 has the same nodal planes as HOMO along z-direction and one mirror plane as symmetry element. This symmetry element facilitates the overlap between both HOMO -4 of PBI1 and PBI2.

HOMO -1 representation has two bumps when $z=4.4$ and $x=8.0 \text{ \AA}$. As in the previous cases, it is due to the overlap between both orbitals.

HOMO -3 has a different behaviour compared to the previous ones in $z=2.4 \text{ \AA}$. This is due to the position of their orbitals, which affects the interaction of both HOMO -3 at this position.

In figure 29 and 30 the overlap of the orbitals named above can be seen.

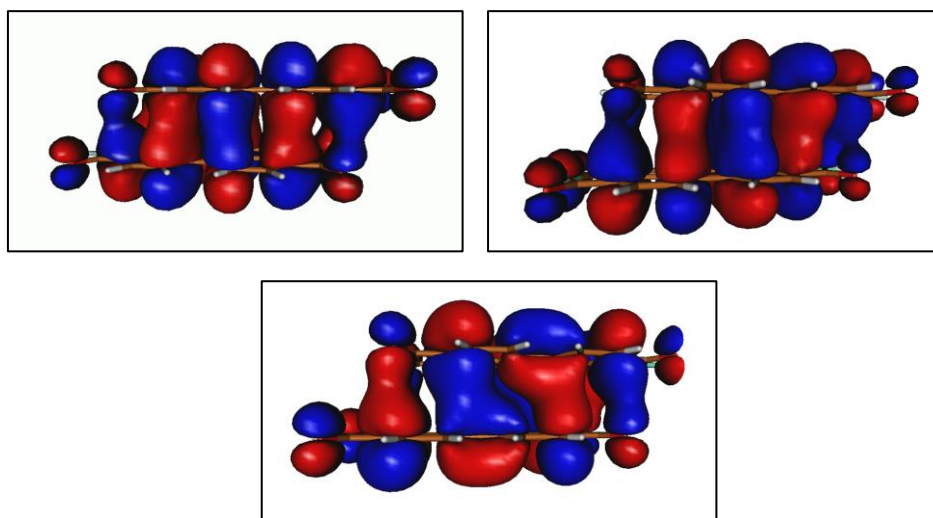


Figure 29: Orbitals overlapped when $z=2.4 \text{ \AA}$. Left: both HOMO. Right: both HOMO -4. Bottom: both HOMO -3.

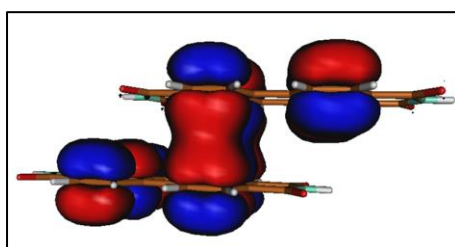


Figure 30: Overlap of both HOMO -1 when $z=4.4 \text{ \AA}$.

Table 2: E_{exr} values (E_h) of each orbital at different points

$z \text{ (\AA)}$	HOMO	HOMO-1	HOMO -3	HOMO -4
2.4	2,89E-03	7,05E-04	3,34E-03	3,90E-03
4.4	2,27E-03	3,44E-03	3,28E-03	2,69E-03
6.8	1,16E-03	7,61E-04	1,65E-03	1,40E-03
9.2	4,18E-04	4,72E-04	6,86E-04	5,04E-04

The E_{exr} values of each orbital in the positions in which figure 28 shows bells can be seen in Table 2.

8.5 Results when PB12 is shifted along the y-axis

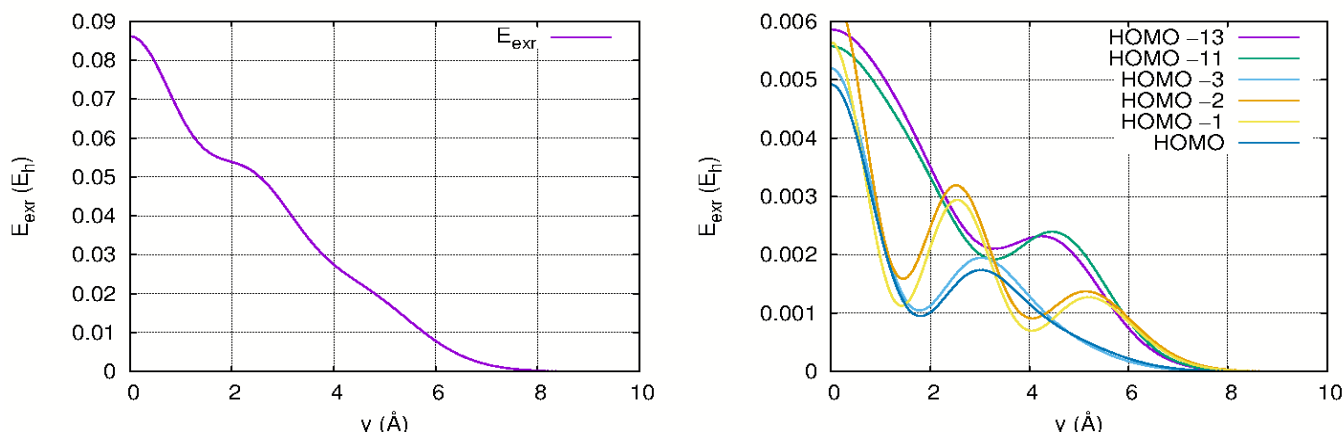


Figure 31: Left: representation of $E_{\text{exr}}(E_h)$ vs distance (\AA) when PB2 is shifted along the y-axis. Right: orbitals which contribute most to the E_{exr} when PB2 is shifted along the y-axis.

The graphic on the left in figure 31, we can see two bumps when $y=2.4$ and 4.8 \AA . The orbitals which show such a pattern as the total E_{exr} represented in the graphic on the right

HOMO has one bump between 2 and 4.4 \AA . It has one node along the y-axis and one mirror plane as symmetry element. The reason for this bump is the same as in the previous cases.

HOMO -3 representation in figure 30 is similar to the HOMO due to the same reason, it also has only one node and there is one mirror plane as symmetry elements. In this region, there is no overlap, then the E_{exr} is 0.

HOMO -1 and HOMO -2 have both two bumps when $x=2.4$ and 4.8 \AA .

HOMO -13 has one bump between 4 and 6 \AA . This orbital has one node on the y-axis.

Again, in this position, there is not interaction between the HOMO -13 orbitals.

HOMO -11 representation in figure 31 is similar to HOMO -13.

The overlap of the previous orbitals named is illustrated in figure 32 and 33 bellow.

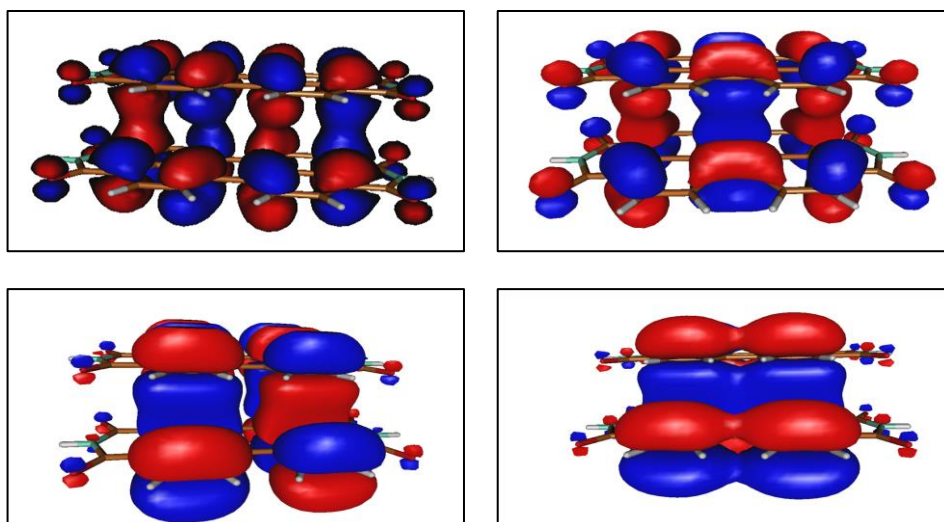


Figure 32: Orbitals overlaped when $y=2.4 \text{ \AA}$. Top left: both HOMO. Top right: both HOMO -3. Bottom left: both HOMO -1. Bottom right: both HOMO -2.

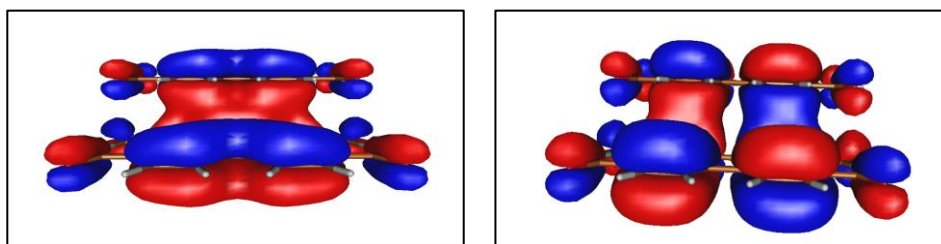


Figure 33: Orbitals overlaped when $y=4.8 \text{ \AA}$. Left: both HOMO -13. Right: both HOMO -11.

Table 3: E_{exr} values (E_n) of each orbital at different points

$y \text{ (\AA)}$	HOMO	HOMO-1	HOMO -2	HOMO -3	HOMO -11	HOMO -13
2.4	1,38E-03	2,88E-03	3,15E-03	1,54E-03	1,09E-03	4,45E-03
4.8	6,64E-04	1,14E-03	1,29E-03	6,65E-04	1,35E-03	6,47E-04

The E_{exr} values of each orbital in the positions in which figure 31 shows maximums can be seen in Table 3.

9. Conclusions

English

- In the N₂-He system:
 - When the He is shifted along the x-axis, the orbitals that contribute most to E_{exr} are: 2σ_g and 1π_{u x}. When it is displaced along the y-axis, 2σ_g and 1π_{u y}.
 - When x and y=4 Å, E_{exr} is approximately 0 (6.26·10⁻⁸ E_h).
- In the Cl₂-He system:
 - When the He is shifted along the x-axis, the orbital that contributes more is 2π_{u x}. When it is displaced along the y-axis, 2π_{u y}.
 - When x and y=4.2 Å, E_{exr} is approximately 0 (6.58·10⁻⁶ E_h).

The basis sets investigated showed that the cc-pVDZ basis generally underestimates E_{exr} by 20%. Furthermore, the TVZP basis is generally a good compromise between basis set size (computational effort) and accuracy. It agrees with more diffuse basis sets like the aug-cc-pVDZ.

In the EDA of both previous systems, it has been proved that E_{exr} is the one that contributes most to the total energy interaction (E_{int}), in both HF and DFT (B-LYP) calculations. The difference is that E_{exr} in DFT calculation has positive values, which differs from its definition, but DFT allows it.

- In the PBI1-PBI2 system:
 - The orbitals that contribute most when PB2 is shifted along the z-axis are: HOMO, HOMO -1, -3 and -4. When it is shifted along the y-axis, HOMO, HOMO-1, -2, -3, -11 and -13. When the orbitals of PBI2 are in the nodes of PBI1, there is not any interaction between the orbitals of both PBIs.

In all cases, the orbitals interactions are the responsible of E_{exr}. The overlap between orbitals is favoured by the symmetry of the system. Furthermore, E_{exr} shows an oscillatory behaviour when the π systems of two PBI molecules are shifted with respect to each other at a constant interplanar distance. The amplitude of the oscillations is approximately 4-6 mE_h for orbital contributions and 10 mE_h for total energies.

Català

- En el sistema N₂-He:
 - Quan l'He és desplaçat al llarg de l'eix x, els orbitals que contribueixen més a l'E_{extr} són: 2σ_g and 1π_{ux}. Quan és desplaçat al llarg de l'eix y, 2σ_g i 1π_{uy}.
 - La distància en què E_{extr} és aproximadament 0 (6.26·10⁻⁸ E_h) correspon a uns valors de x i y de 4 Å.
- En el sistema Cl₂-He:
 - Quan l'He és desplaçat al llarg de l'eix x, l'orbital que contribueix més és 2π_{ux}. Quan és desplaçat al llarg de l'eix y, 2π_{uy}.
 - La distància en què E_{extr} és aproximadament 0 (6.58·10⁻⁶ E_h) correspon a uns valors de x i y=4.2 Å.

En l'EDA de tots dos sistemes anteriors s'ha comprovat l'E_{extr} és l'energia que contribueix més a l'energia total d'interacció (E_{int}), tant en el càlcul HF com en DFT (B-LYP). La diferència d'ambdós càlculs és que l'E_{extr} en DFT té valors positius, la qual cosa difereix de la seva definició, però el càlcul DFT ho permet fer.

Els conjunts de bases investigats han mostrat que la base cc-pVDZ generalment subestima l'E_{extr} en un 20%. A més, la base de TVZP mostra en general un bon compromís entre la mida de conjunt de base (esforç computacional) i la precisió. Mostra resultats semblants a conjunts de bases més difusos com l'aug-cc-pVDZ.

- En el sistema PBI1-PBI2
 - Els orbitals que contribueixen més quan PBI2 es desplaça al llarg de l'eix z són: HOMO, HOMO -1,-3 i -4. Quan es desplaça al llarg de l'eix y, HOMO, HOMO-1,-2,-3,-11 i -13. Quan els orbitals de la PBI2 es situen en regions de PBI1 on hi ha nodes, no hi ha interacció entre els orbitals d'ambdues PBI.

En tots els casos, les interaccions dels orbitals són les responsables de l'E_{extr}. El solapament d'orbitals es veu afavorit per la simetria que presenta el sistema. A més, E_{extr} mostra un comportament oscil·latori quan els sistemes π de les molècules de PBI es desplacen entre si a una distància interplanar constant. L'amplitud de les oscil·lacions és d'aproximadament de 4-6 mE_h per a les contribucions dels orbitals i 10 mE_h per a les energies totals.

10. Bibliography

- [1] Cabrera Acosta, D.; Gutiérrez Díaz, J.A. Fuentes de energía y su impacto en el medioambiente. Universidad de Ciencias Pedagógicas, La Habana. Available at: <http://www.cubasolar.cu/biblioteca/ecosolar/Ecosolar56/HTML/articulo06N.html>. (Accessed: 19th April 2018)
- [2] Computational Chemistry for a Sustainable Future: Dye-Sensitized Solar Cells | YourFormula. Available at: <http://archive.yourformula.eu/internalposts/computational-chemistry-for-a-sustainable-future-dye-sensitized-solar-cells/>. (Accessed: 19th April 2018)
- [3] Jensen, F. *Introduction to Computational Chemistry*, 2; John Wiley & Sons Ltd: England, 2007; pp 19, 80-82, 192-198, 248-249.
- [4] Sherrill, C. D. The Hartree-Fock Equations. Available at: <http://vergil.chemistry.gatech.edu/notes/hf-intro/node7.html>. (Accessed: 25th April 2018)
- [5] Stone, A. J. *The Theory of Intermolecular Forces*, 3; Oxford University Press: Oxford, 2002; 32; pp 4, 74-75, 81, 96.
- [6] Sherrill, C. D. Basis Sets in Quantum Chemistry. Available at: <http://vergil.chemistry.gatech.edu/courses/chem6485/pdf/basis-sets.pdf> (Accessed: 25th April 2018)
- [7] Henrichsmeyer, J.; Winkler, M.; Fink, R. F. Orbital pair contributions to the exchange-repulsion energy between closed-shell atoms and molecules, unpublished.
- [8] a/ Su, P. and Li, H. Energy decomposition analysis of covalent bonds and intermolecular interactions. *J. Chem. Phys.* **131**, 014102 (2009).
- b/ Electrostatic interaction | Article about Electrostatic interaction by The Free Dictionary. Available at: <https://encyclopedia2.thefreedictionary.com/Electrostatic+interaction>. (Accessed: 12th May 2018)
- [9] Grimme, S. Do special noncovalent π - π stacking interactions really exist? *Angew. Chemie - Int. Ed.* **47**, 3430–3434 (2008).
- [10] Fink, R. F.; Seibt, J.; Engel, V.; Renz, M.; Kaupp, M.; Lochbrunner, S.; Zhao, H-M.; Pfister, J.; Würthner, F. and Engels, B. Exciton trapping in π -conjugated materials: A quantum-chemistry based protocol applied to perylene bisimide dye aggregates. *J. Am. Chem. Soc.* **130**, 12858–12859 (2008).
- [11] Zhao, H. M. *et al.* Understanding ground- and excited-state properties of perylene tetracarboxylic acid bisimide crystals by means of quantum chemical computations. *J. Am. Chem. Soc.* **131**, 15660–15668 (2009).

Appendix

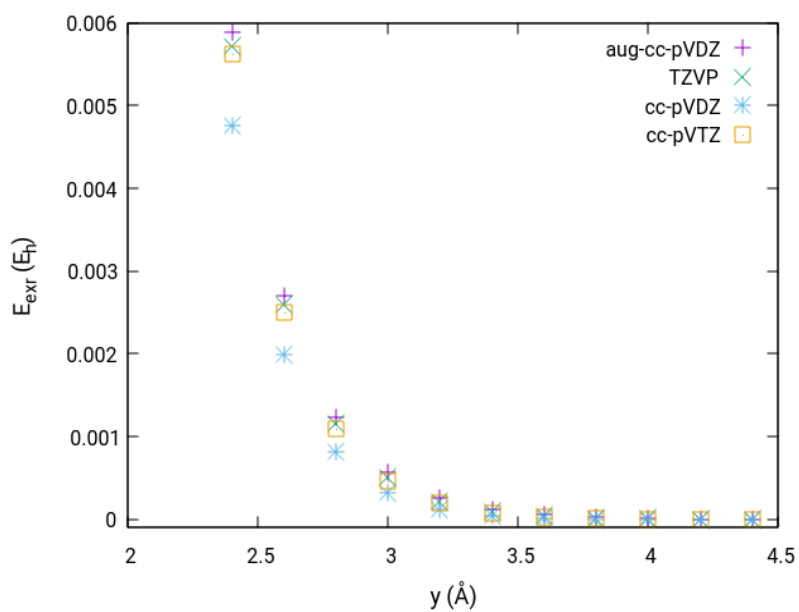


Figure 34: $\text{N}_2\text{-He}$, representation of basis sets behaviour when He is shifted on the y-axis.

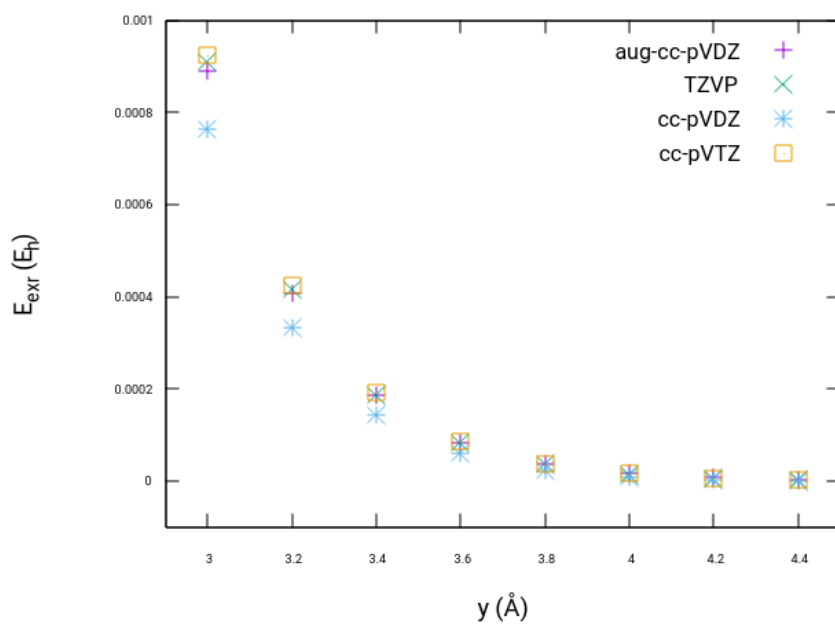


Figure 35: $\text{Cl}_2\text{-He}$, representation of basis sets behaviour when He is shifted on the y-axis.

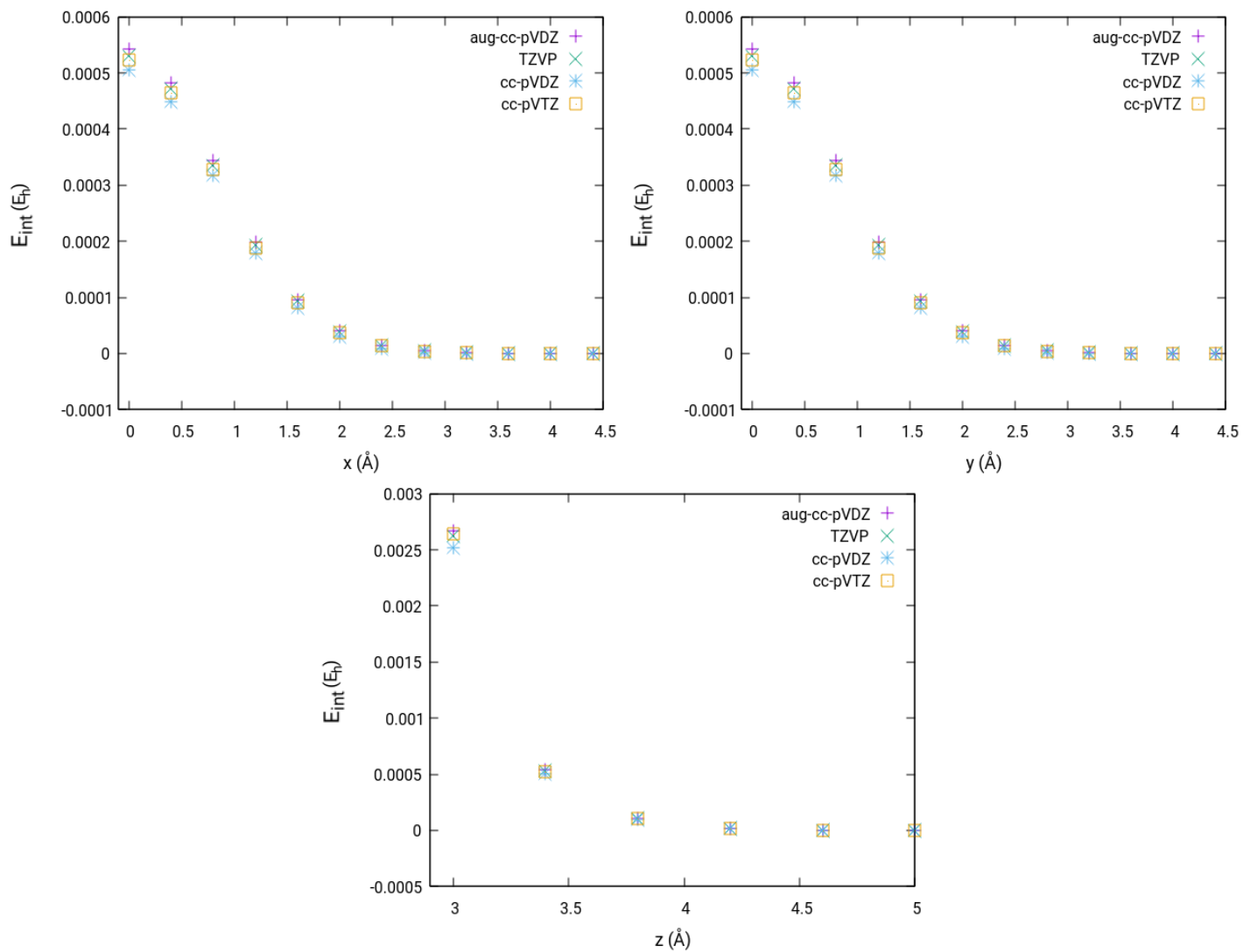


Figure 36: N_2 -He HF,EDA representation of basis sets behaviour. Right: when He is shifted on the x-axis. Left: when He is shifted on the y-axis. Bottom: when He is shifted on the z-axis.

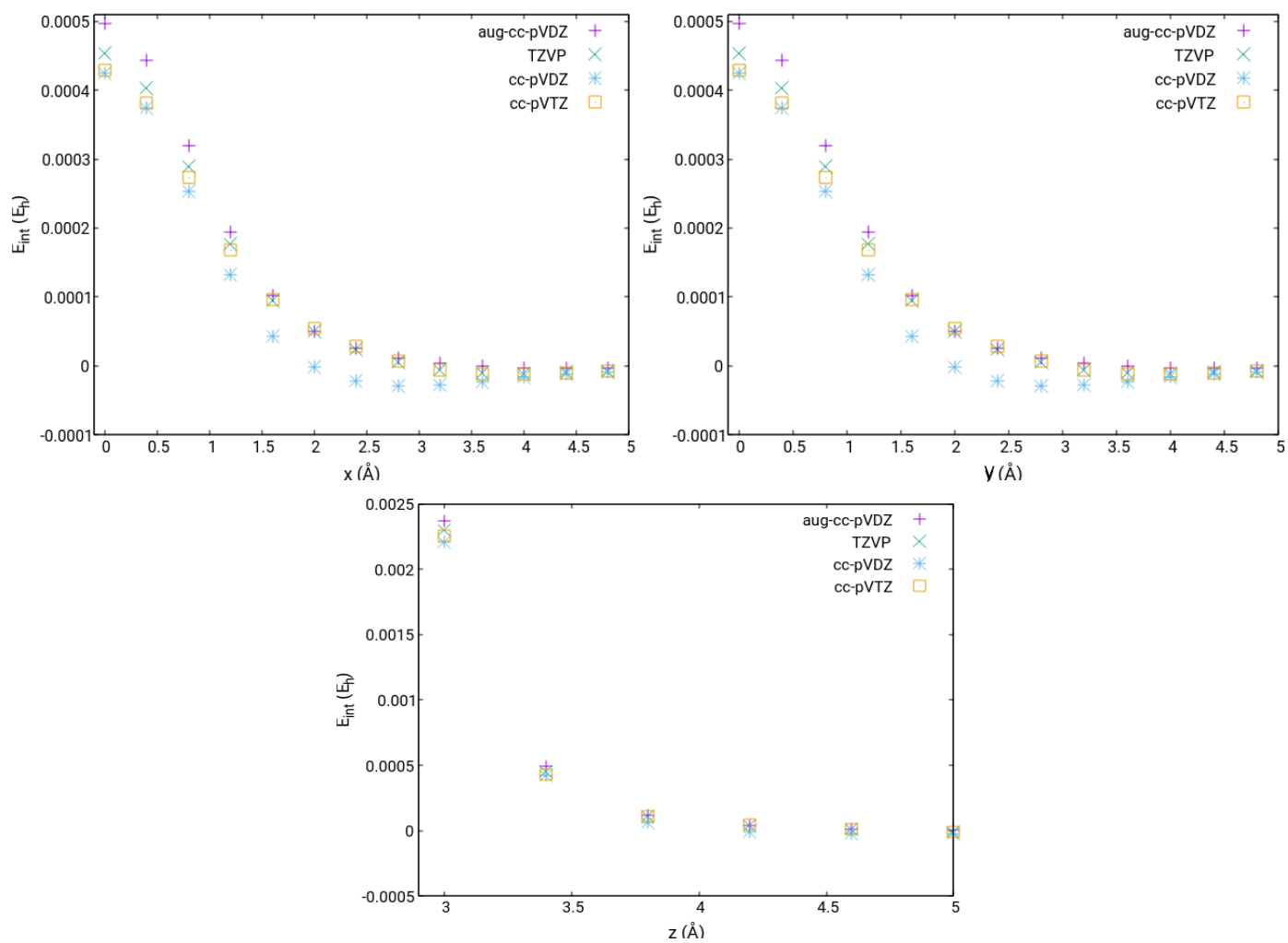


Figure 37: $\text{N}_2\text{-He}$, B-LYP,EDA representation of basis sets behaviour. Left: when He is shifted on the x-axis. Right: when He is shifted on the x-axis. Bottom: when He is shifted on the z-axis.

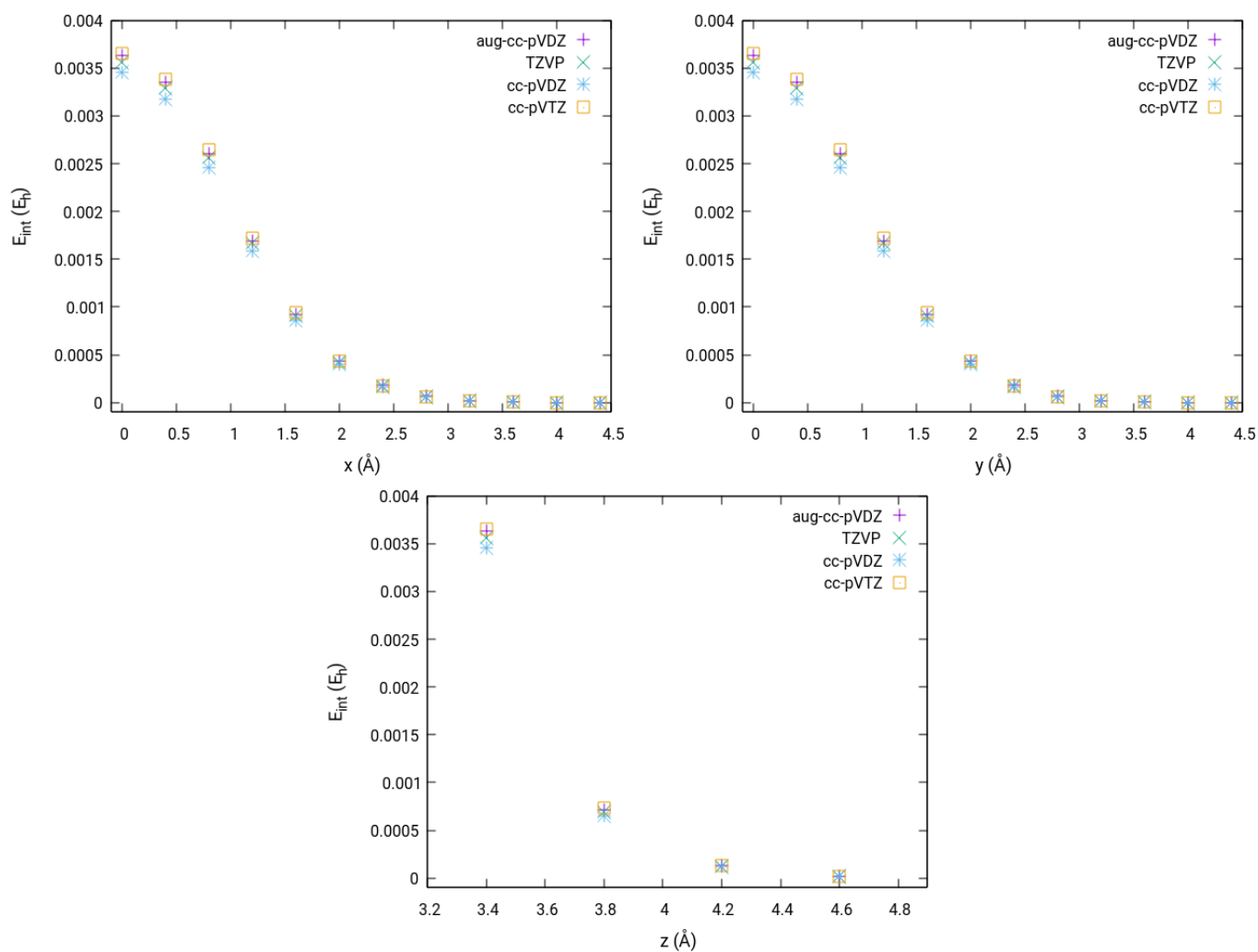


Figure 38: $\text{Cl}_2\text{-He}$, HF, EDA representation of basis sets behaviour. Left: when He is shifted on the x-axis. Right: when He is shifted on the y-axis. Bottom: when He is shifted on the z-axis.

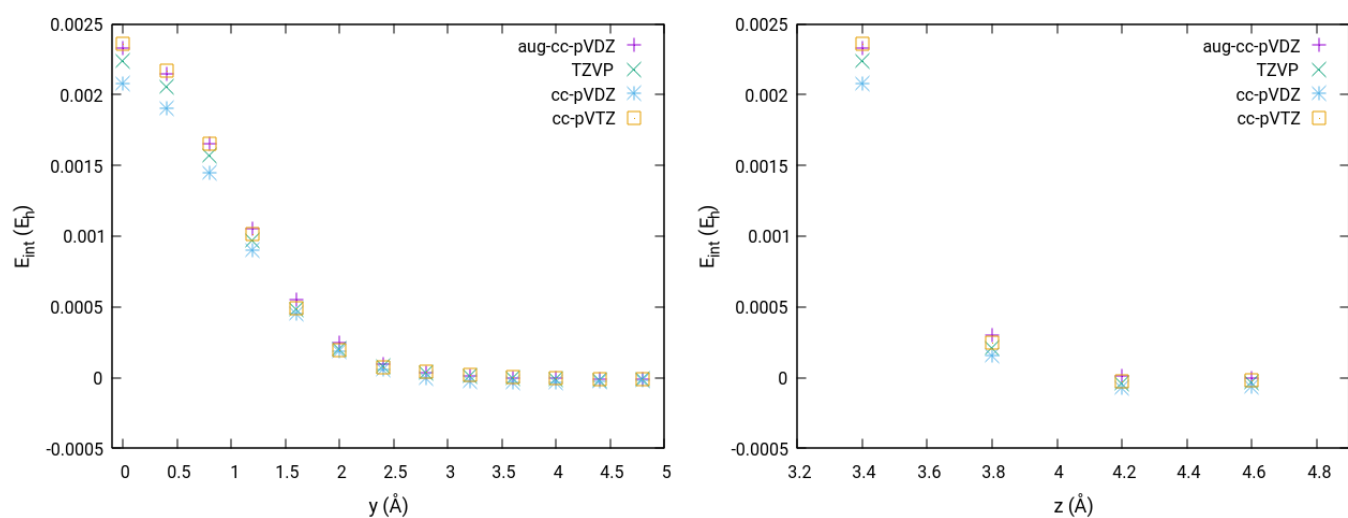


Figure 39: $\text{Cl}_2\text{-He}$, B-LYP, EDA representation of basis sets behaviour. Left: when He is shifted on the y-axis. Right: when He is shifted on the z-axis.

Acknowledgements

English

I want to thank all the people who helped me make this thesis possible:

First of all, I want to thank Prof. Dr Reinhold F. Fink for welcoming me in his research group and introducing me to this interesting topic for my thesis. I also want to thank him for all the resources, such as books and papers, that he recommended me. Furthermore, I do appreciate every time he helped me with any problem I had.

I thank Jihene Jerbi for introducing me to this research project, for helping me whenever I had a question and for encouraging me to do this work.

I also want to thank Stefan Behnle for solving always my problems with my calculations and with the computer operation.

Thanks to Prof. Dr. Ma Elena Fernández Gutiérrez, coordinator of this ERASMUS, who made this experience possible. I would also like to thank all the chemistry professors at the Universitat Rovira i Virgili, who taught me everything I know about chemistry.

Thanks to my friend Naia Morancho Marzal, who always made me feel lively and who also encouraged me to do this thesis.

Finally, I also want to thank my family. Even though we are in different countries, they always supported me to do this thesis. Thank you for all your efforts so that I could study chemistry.

Català

Vull agrair a totes les persones que m'han ajudat a fer possible aquest treball:

En primer lloc, vull agrair al Prof. Dr. Reinhold F. Fink per donar-me la benvinguda al seu grup de recerca i introduir-me en aquest interessant tema per fer el meu treball. També vull donar-li les gràcies per tots els recursos, com ara llibres i articles, que m'ha recomanat. A més, li estic molt agraïda per ajudar-me sempre amb qualsevol problema.

Agraeixo a Jihene Jerbi que m'hagi introduït al seu projecte d'investigació, per ajudar-me cada vegada que tenia una pregunta i per animar-me a fer aquest treball.

També vull donar les gràcies a Stefan Behnle per resoldre sempre els meus problemes amb els càlculs i amb el funcionament de l'ordinador.

Gràcies a la Prof. Dra. Ma Elena Fernández Gutiérrez, coordinadora d'aquest ERASMUS, qui ha fet possible aquesta experiència. També vull donar les gràcies a tots professors de química de la Universitat Rovira i Virgili, que m'han ensenyat tot el que sé de química.

Gràcies a la meva amiga Naia Morancho Marzal, qui sempre m'ha transmès la seva energia i qui també m'ha animat a fer aquest treball.

Finalment, també vull donar les gràcies a la meva família. Encara que estiguem en diferents països, sempre m'han recolzat per fer aquest treball. Gràcies per tots els esforços perquè pogués estudiar química.